NOAA Technical Report ERL 425-WPL 58

Signal Processing and Range Spreading in the FM-CW Radar

Edmond A. Costa
Russell B. Chadwick

May 1984

U.S. DEPARTMENT OF COMMERCE
National Oceanic and Atmospheric Administration
Environmental Research Laboratories

NOAA Technical Report ERL 425-WPL 58

Signal Processing and Range Spreading in the FM-CW Radar

Edmond A. Costa
Russell B. Chadwick

Wave Propagation Laboratory

May 1984

U.S. Department of Commerce
Malcolm Baldrige, Secretary

National Oceanic and Atmospheric Administration
John V. Byrne, Administrator

Environmental Research Laboratories
Boulder, Colorado
Vernon E. Derr, Director

CONTENTS

Signal Processing and Range Spreading in the FM-CW Radar

Edmond A. Costa and Russell B. Chadwick

ABSTRACT. One- and two-dimensional methods of processing data from the FM/CW radar, through use of Discrete Fourier Transforms, are shown to be subject to the undesirable effect of "range spreading", in which power associated with a particular range cell is smeared into other range cells because of high sidelobes on the range spectrum, thereby interfering with velocity spectra associated with other range cells. Efforts to solve the problem are described; weighting the data produces promising results; results of ad hoc methods of smoothing are less promising.

1. INTRODUCTION

Radars capable of receiving returns from optically clear air have been used on a research basis for nearly two decades. These radars receive electromagnetic waves scattered by half-wavelength refractive-index fluctuations in the clear atmosphere. The fluctuations are due to atmospheric turbulence and are present virtually all the time. The fact that clear-air returns exist almost all the time presents the opportunity for an all-weather wind-sensing capability. A system to measure winds continuously over a given volume of the atmosphere would find wide use.

Clear-air radars will soon be used operationally for a number of different applications (Chadwick and Gossard, 1983). In addition to its research activities involving wind measurements up to 100 km altitude, the National Weather Service is evaluating a system of large clear-air radars looking vertically to measure wind profiles for use in weather prediction. The same system of radars that measures wind profiles around the country can provide information to route commercial aircraft to minimize fuel consumption. It could also provide information for tracking and predicting trajectories of wind-borne pollution such as acid rain or nuclear contamination.

Other types of clear-air radar may find use at airports as a hazard detector. It is well established that clear-air radars can detect both hazardous wind shear and hazardous wake turbulence. Furthermore, it appears feasible to develop radars that detect these hazards in terminal areas under all weather conditions.

The FM-CW clear-air radar is unique in that it can operate at exceedingly short ranges where other types of radars are saturated by clutter. Richter (1969) originated the idea of using an FM-CW radar to study clear-air phenomena in the atmosphere. He operated in a range-only mode looking vertically with range resolution on the order of a meter. The resulting pictures of clear-air

layers provided much new information on the structure of the planetary boundary layer. Chadwick et al. (1976) developed Doppler capability for an FM-CW radar and showed that a short-range radar could be used to measure wind in the lower atmosphere. Recently, Gossard et al. (1982) showed that this same type of radar could be used to measure refractive-index gradients and hence be useful for determining radar coverage. To do this requires that the radar be capable of measuring the zeroth, first, and second moments of the velocity spectrum. To understand possible sources of error and to determine limits on any fundamental errors inherent in FM-CW radars, it was necessary to perform a thorough study and computer simulation of the signal processing used to derive velocity spectra in an FM-CW radar. In previous work, Barrick (1973) and Chadwick et al. (1981) had noted the need for time weighting of the signal prior to determining the range-ordered power spectra. This is like conventional weighting to reduce the effects of discontinuities at the start and end of the data, but there is an important difference in that there are discontinuities at regular intervals in the data. These discontinuities are a natural consequence of the reset interval of the microwave signal source and cannot be eliminated. Signal processing offers means of compensation.

2. FM-CW RADAR: PRINCIPLES OF OPERATION

2.1 Transmitted Signal

The FM-CW radar uses two antennas, one for receiving and one for transmitting. The transmitted signal has a linear frequency sweep or "chirp". That is, it is initially set at f_o and then swept linearly in time to a frequency $f_o + B$ (B being the bandwidth of the sweep) and then reset to f_o before being swept again. In Fig. 2.1, it is seen that the frequency is swept for T seconds before being reset, the rate of sweep being held constant (that is, df/dt = B/T). There may be a dead time before the next sweep begins. The total time from the start of one sweep to the start of the next sweep is defined as G. In general G does not equal T, and in practice cannot be due to the finite interval of time it takes to reset the signal to f_o.

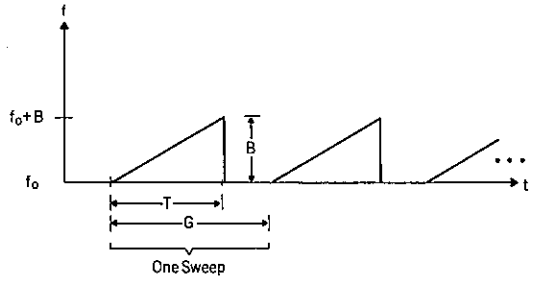

Figure 2.1.--Frequency characteristics of the transmitted signal plotted as a function of time. The frequency is swept from f_o to $f_o + B$ in T seconds and then returned to f_o. The sweep is repeated every G seconds.

For convenience and reasons that will be apparent later, t_n is defined as the time elapsed since the start of the nth sweep. That is, the independent variable t, which is time, is

$$t = n\,G + t_n \tag{2.1}$$

where n is the number of sweeps since an arbitrary reference time (t = 0). So if

$$n\,G < t < (n+1)G\ ,$$

then the nth sweep is being transmitted.

By use of this convention, the transmitted signal can be expressed as

$$S_T(n,t_n) = A\cos 2\pi\left[\left(f_o + \frac{B}{2T}\,t_n\right)t_n + \phi_n\right] \qquad \text{for} \quad 0 \leqslant t_n \leqslant T \tag{2.2}$$

where ϕ_n is some initial phase of the signal. Note that $S_T(n,t_n)$ is identical for all n. That is, the same signal is repeated every G seconds. This is critical to the retrieval of the velocity information of a target.

2.2 Received Signal

Some of the energy of the transmitted signal will be reflected by a target and collected by the receiving antenna. The received signal due to one target is just the transmitted signal delayed in time by τ (round trip time of signal from radar to target and back) and attenuated by some factor. The expression for the received signal is

$$S_R(n,t_n) = \bar{A}\cos 2\pi\left\{\left[f_o + \frac{B}{2T}(t_n - \tau)\right](t_n - \tau) + \phi_n\right\} \qquad \text{for} \quad \tau \leqslant t \leqslant +T + \tau\ . \tag{2.3}$$

The key thing to note about the received signal is the time delay τ relative to the transmitted signal. It is this delay τ that contains the range and velocity information of the target. In general τ is a function of time, and can be approximated as

$$\tau \approx \frac{2R}{c}$$

where R is the range of the target. The time dependence of τ is due to the fact that range may be a function of time because of the movement of the target. It is assumed that the target is moving at a constant velocity (v) during the observation interval. Then,

$$R = R_o + vt$$

where R_o is the initial range of target at t = 0, or at the instant the first sweep begins. So,

$$\tau = \frac{2R_o}{c} + \frac{2v}{c} t \ .$$

Thus, τ is a function of the initial range of the target and the velocity of the target. Note that the term (2v/c)t is the Doppler effect of the moving target on the signal.

When t is expressed in terms of n and t_n through the use of Eq. (2.1), τ can be expressed as follows:

$$\tau = \frac{2R_o}{c} + \frac{2v}{c} n\ G + \frac{2v}{c} t_n. \qquad (2.4)$$

This equation states that τ changes continuously during a sweep because of $(2v/c)t_n$ term, and changes in increments from sweep to sweep because of the n (2v/c)G term. For a constant t_n, the latter term is totally responsible for any change in τ. Thus, knowing the rate of change of τ from sweep to sweep is the same as knowing the value of this term, which can be used to determine the velocity of the target. Once the velocity is known, R_o can be determined exactly since it is the only other unknown in Eq. 2.4.

Therefore, the problem of recovering velocity and range information from the received signal is the determination of τ. To see how this may be accomplished consider Fig. 2.2, where frequency vs. time is plotted for the transmitted and received signals. From the plot it can be seen that the received

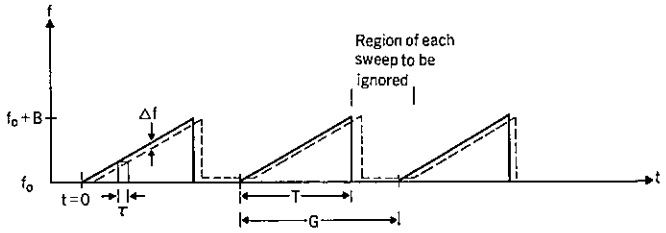

Figure 2.2.--Frequency characteristics of the transmitted and received signals plotted as a function of time. The solid line corresponds to the transmitted signal; the broken line corresponds to the received signal.

signal is shifted relative to the transmitted signal, and that this shift of τ is directly related to the difference in frequency (Δf) between the two signals at any given instant. This suggests that knowledge of Δf can be used to determine τ and thereby determine range and velocity. (At this point it is appropriate to mention that the region of interest is $\tau \leqslant t_n \leqslant T$. It is in this interval that the transmitted and received signals will be correlated to find Δf; data outside this interval will be ignored.)

A standard method of determining Δf is to mix the received signal with a replica of the transmitted signal and then to low-pass filter the result. After mixing the low-pass filtering the following signal is available for processing (see the Appendix for derivation):

$$x(n,t_n) = \cos 2\pi \left\{ \left[f_o\left(\frac{2v}{c}\right) + \frac{B}{T}\left(\frac{2R_o}{c}\right) \right] t_n + n\, f_o\left(\frac{2v}{c}\right) G + f_o\left(\frac{2R_o}{c}\right) \right\} . \qquad (2.5)$$

(1) The frequency present during a sweep is

$$f_o\left(\frac{2v}{c}\right) + \frac{B}{T}\left(\frac{2R_o}{c}\right) .$$

(2) There is a phase change from sweep to sweep due only to the velocity:

$$n\, f_o\left(\frac{2v}{c}\right) G .$$

(3) There is a constant-phase term

$$f_o\left(\frac{2R_o}{c}\right) .$$

The velocity can be obtained by finding the phase shift from sweep to sweep. For this reason it is important that f_o not change greatly from sweep to sweep, so that fluctuations of the constant-phase term do not interfere with or mask the $nf_o(2v/c)G$ term.

To obtain the velocity information, consider holding t_n constant, or viewing $x(n,t_n)$ at the same value of t_n during each sweep. That is,

$$x(n,t_n = k) = \cos 2\pi \left(n\, f_o \frac{2v}{c} G + \theta \right), \tag{2.6}$$

where

$$\theta = f_o \frac{2R_o}{c} + \left(f_o \frac{2v}{c} + \frac{B}{T} \frac{2R_o}{c} \right) k$$

does not change from sweep to sweep. Eq (2.6) is just a discrete time signal, or the sampled version of the continuous time signal

$$x(t) = \cos 2\pi (f_o \frac{2v}{c} t + \theta) \quad ;$$

n is the sample index; G is the sampling interval; and f_o $(2v/c)$ is the frequency of the signal. A DFT (Discrete Fourier Transform) can be used to obtain the spectrum (and therefore the velocity information) of the discrete time signal.

Likewise, if n is held constant (that is, only one sweep is considered) a Fourier Transform can be applied to $x(n = k,t_n)$ to yield a spectrum from which f_o $(2v/c)$ + B/T $(2R_o/c)$ can be obtained. From this the range can be determined.

To summarize:

(1) The rate of change of the phase of the mixed signal from one sweep to the next is due to the velocity of the target.

(2) The range of the target is obtained from knowing the rate of change of the phase of the mixed signal during a sweep.

2.2.1 Discrete Time Signal

After the signal $x(n,t_n)$ is obtained from the mixer it must be processed to yield the range and velocity information. Generally, signal processing is

done digitally. So, prior to processing, the continuous time signal is sampled to provide a discrete time signal. That is, the signal will be sampled at discrete values of t_n. The sampling rate is defined as f_s; therefore, the signal will be sampled once every $1/f_s$ seconds, and m will be the sample index.

The sampled signal is

$$x(n,m) = x\left(n, t_n = m\frac{1}{f_s}\right)$$

$$x(n,m) = \cos 2\pi\left\{\left[f_o\left(\frac{2v}{c}\right) + \frac{B}{T}\left(\frac{2R_o}{c}\right)\right]\frac{m}{f_s} + n\,G\,f_o\left(\frac{2v}{c}\right) + f_o\left(\frac{2R_o}{c}\right)\right\} \qquad (2.7)$$

$$0 \leqslant n \leqslant N-1 \quad ,$$

$$0 \leqslant m \leqslant M-1 \quad .$$

For convenience the signal can be rewritten as

$$x(n,m) = \cos 2\pi\ (m\omega^r + n\omega^v + \phi) \qquad (2.8)$$

where

$$\omega^r = \frac{1}{f_s}\left[f_o\left(\frac{2v}{c}\right) + \frac{B}{T}\left(\frac{2R_o}{c}\right)\right] \quad ,$$

$$\omega^v = G\,f_o\left(\frac{2v}{c}\right) \quad ,$$

$$\phi = f_o\left(\frac{2R_o}{c}\right) \quad ,$$

and the superscripts r and v on ω^r and ω^v were chosen to denote the underlying dependence these terms have on range and velocity respectively.

2.2.2 Sampling Considerations

The function x(n,m) of Eq. (2.7) was formed by taking samples of a continuous time function. From the sampling theorem it is known that the sampling rate must exceed twice the maximum frequency present in the signal being

sampled; otherwise "aliasing" will occur. This implies that $1/f_s$ and G in Eq. (2.7) determine the maximum range and velocity a target can have and still be interpreted correctly by the radar. The relationships are as follows:

$$\frac{1}{G} > 2\, f_o\, \frac{2v}{c} \rightarrow v < \frac{1}{G}\, \frac{c}{4f_o}$$

and

$$f_s > 2 \left[f_o \left(\frac{2v}{c}\right) + \frac{B}{T} \left(\frac{2R_o}{c}\right) \right] \quad .$$

In practice, the inequality for f_s can be guaranteed when the continuous time signal is low-pass filtered at the output of the mixer. This would be just prior to sampling $x(n,t_n)$ to form $x(n,m)$. The inequality on G, however, is not as easy to guarantee. The radar gathers data along this dimension (n) at discrete intervals of time. Therefore, there was never any continuous time signal to low-pass filter before sampling. When G is chosen, the maximum expected velocity of the target becomes the constraint.

3. BASIC SIGNAL PROCESSING

As pointed out in sec. 2, the range* of a target can be determined if the frequency of the signal x(n,m) is known for a constant n, and the velocity of the target can be determined if the frequency of the signal x(n,m) is known for a constant m. That is, the rate of change of phase during a sweep contains the range information, and the rate of change of phase from sweep to sweep contains the velocity information. This applies for one discrete target. If more than one target is present, however, the spectrum of a sweep (a row of x(n,m)) will provide information from which the range of each target can be determined, and the spectrum from sweep to sweep (a column of x(n,m)) will yield the velocities of all the targets, but it will not be possible to associate a given velocity with a particular range.

There are, however, ways to associate both range and velocity with the same target when more than one target is present. This chapter will discuss

*Recall from Eq. (2.8) that it is ω^r that can be found from which the range can then be calculated. It should be noted that velocity also contributes to ω^r, and this must be taken into account.

two possible methods. Both methods employ the DFT (Discrete Fourier Transform) as the standard tool to obtain the spectrum of a discrete sequence. The use of the DFT is convenient, especially when it is desired to process the information in real time, because there are algorithms that can perform a DFT efficiently and quickly, the most common being the FFT (Fast Fourier Transform).

The first method will be referred to as the two-dimensional method. Of the two methods it is perhaps the more intuitively obvious. It consists of treating the function x(n,m) as an N × M array of data, n being the row index and m being the column index. The first step is to perform a DFT on each row of the matrix, and replace each row with the corresponding values obtained from the DFT. The result of replacing all the rows of the matrix with their DFT will be a matrix of complex numbers, and a DFT can then be performed on each column of the matrix. The magnitude squared of the result is then taken to give the two-dimensional power spectrum of the array x(n,m). From this spectrum the range, velocity, and relative radar cross sections of different targets can be obtained.

When the first set of DFT's was applied to the rows of the matrix x(n,m), it was applied to real numbers. The result was a complex sequence, which is conjugate symmetric. That is, half the sequence is just the complex conjugate of the other half. The second set of DFT's is applied to these complex numbers; in this case the result is not constrained to be conjugate symmetric, and negative frequencies can be distinguished from positive frequencies. This permits determining whether ω^{∇} (and therefore velocity) is positive or negative.

The second method will be referred to as the one-dimensional method. This method is implemented by performing an NM-point DFT over the sequence created by placing each sweep immediately after the previous sweep, as illustrated in Fig. 3.1. After the DFT is performed the magnitude squared of the result is taken. This is the power spectrum of the above long sequence that was created by stacking sweeps end to end. Once again range, velocity, and relative radar cross section can be determined for different targets from this power spectrum.

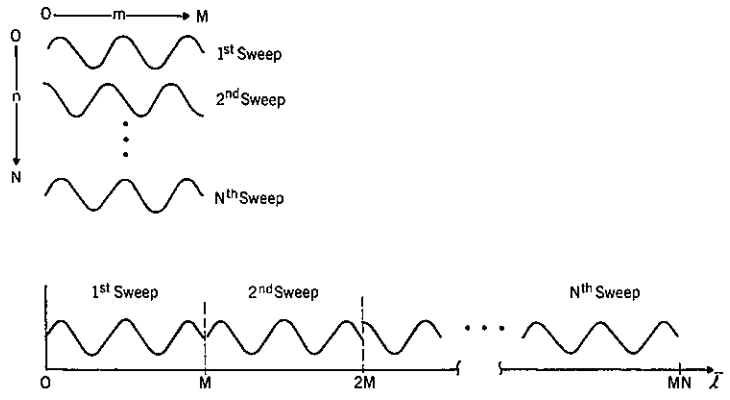

Figure 3.1.--2-D method (above) and 1-D method (below) of treating data from the radar. In the 2-D method a two-dimensional DFT is performed on the N × M array. In the 1-D method an MN-point DFT is applied over the sequence composed of all the data.

3.1 Two-Dimensional Method

The following is a development of how to obtain the velocity and range of a target by applying a two-dimensional DFT to the signal. The development is carried out for one discrete target, but from the nature of the final result it will be seen that the method will work for multiple targets also.

The radar signal for one discrete target is repeated for convenience:

$$x(n,m) = \cos 2\pi(m\omega^r + n\omega^v + \phi) \qquad \begin{matrix} 0 \leqslant n \leqslant N-1 \\ 0 \leqslant m \leqslant M-1 \end{matrix} \qquad (3.1)$$

where

$$\omega^r = \frac{1}{f_s}\left[\frac{B}{T}\left(\frac{2R_o}{c}\right) + f_o\left(\frac{2v}{c}\right)\right]$$

$$\omega^v = f_o\left(\frac{2v}{c}\right) G$$

$$\phi = f_o\left(\frac{2R_o}{c}\right).$$

By definition (Rabiner and Gold, 1975, p. 449) the two-dimensional DFT is

$$X(k,\ell) = \frac{1}{NM}\sum_{n=0}^{N-1}\sum_{m=0}^{M-1} x(n,m)\, e^{-j2\pi mk/M}\, e^{-j2\pi n\ell/N} \quad . \qquad (3.2)$$

This is simply a DFT applied in one dimension and then a second DFT applied in the other dimension over the results of the first DFT. The order in which the DFT's are applied is irrelevant. (Mathematically this is equivalent to switching the order of the summations in the above expression.) For the FM-CW the implication is that it makes no difference whether the rows or columns of $x(n,m)$ are processed first.

Applying the two-dimensional DFT to the radar equation gives the following:

$$X(k,\ell) = \frac{1}{NM}\sum_{n=0}^{N-1} e^{-j2\pi n\ell/N} \sum_{m=0}^{M-1} \cos 2\pi(m\omega^r + n\omega^v + \phi)\, e^{-j2\pi mk/M} \quad . \qquad (3.3)$$

Evaluating the right-hand side of the above expression and taking the magnitude squared gives

$$|X(k,\ell)|^2 = \frac{1}{(NM)^2}\ \frac{1}{4}\left[\frac{\sin N\pi(\omega^v - \ell/N)\ \sin M\pi(\omega^r - k/M)}{\sin\pi(\omega^v - \ell/N)\ \sin\pi(\omega^r - k/M)}\right]^2$$

$$+\ \frac{1}{(NM)^2}\ \frac{1}{4}\left[\frac{\sin N\pi(\omega^v + \ell/N)\ \sin M\pi(\omega^r + k/M)}{\sin\pi(\omega^v + \ell/N)\ \sin\pi(\omega^r + k/M)}\right]^2$$

$$+\ \frac{1}{2}\ \frac{1}{(NM)^2}\left\{\frac{\sin N\pi(\omega^v - \ell/N)\ \sin N\pi(\omega^v + \ell/N)\ \sin M\pi(\omega^r - k/M)\ \sin M\pi(\omega^r + k/M)}{\sin\pi(\omega^v - \ell/N)\ \sin\pi(\omega^v + \ell/N)\ \sin\pi(\omega^r - k/M)\ \sin\pi(\omega^r + k/M)}\right.$$

$$\left.\times\ \cos 2\pi[\omega^v(N-1) + \omega^r(M-1) + 2\phi]\right\}. \qquad (3.4)$$

Eq. (3.4) defines samples of a normalized two-dimensional frequency spectrum of a two-dimensional discrete time signal. One of its properties is that it is periodic in ℓ every N samples and periodic in k every M samples. Therefore, it is necessary to consider the above function only for

$$-\frac{N}{2} \leqslant \ell \leqslant \frac{N}{2} \qquad \text{and} \qquad -\frac{M}{2} \leqslant k \leqslant \frac{M}{2}\ .$$

The recurring term of the expression is of the form $\sin N\pi x/\sin\pi x$. A graph of this function is shown in Fig. 3.2. In Eq. (3.4) $x = \ell/n \pm \omega^v$ or $x = k/M \pm \omega^r$, so it is seen that ω^r and ω^v determine the positioning of the function relative to $\ell = 0$ or $k = 0$.

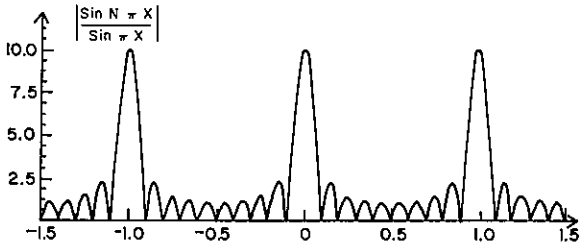

Figure 3.2a.--Representation of $|\sin N\pi x/\sin\pi x|$. For this example N = 10. Mainlobe width = 0.2, sidelobe width = 0.1. The number of sidelobes depends on N.

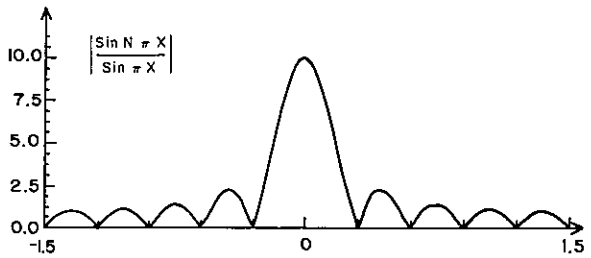

Figure 3.2b.--Representation of $|\sin N\pi x/\sin\pi x|$ for one period. In this case N = 10. Therefore, the maximum amplitude is 10, and the mainlobe has N/2 - 1 associated sidelobes on each side of the center.

The first term of Eq. (3.4) is

$$\left[\frac{\sin N\pi(\omega^v - \ell/N)\ \sin M\pi(\omega^r - k/M)}{\sin\pi(\omega^v - \ell/N)\ \sin\pi(\omega^r - k/M)}\right]^2 .$$

Its maximum occurs when k and ℓ are such that they are both sampling their respective maximums (or close to it). That is, the term is maximum when $\ell = N\omega^v$ and $k = M\omega^r$. Therefore, ω^r and ω^v can be determined, provided the location of this peak is distinguishable. Then range and velocity can be calculated from ω^v and ω^r.

The maximum of this first term will always be located for $0 \leq k \leq M/2$ because ω^r is always positive. (Recall that ω^r is primarily dependent on R_o which is always positive. It does, however, also have a dependence of v, which can be negative. Therefore, for very small R_o, ω^r may go negative if v does.) For the same reason, the maximum of the second term of Eq. (3.4),

$$\left[\frac{\sin N\pi(\omega^v + \ell/N)\ \sin M\pi(\omega^r + k/M)}{\sin\pi(\omega^v + \ell/N)\ \sin\pi(\omega^r + k/M)}\right]^2 ,$$

will always be located when $-M/2 \leq k \leq 0$. Therefore the peaks due to both of these terms are always distinguishable from each other except at $\omega^r = 0$ where they reinforce each other. Of course the sidelobes associated with either of these terms will interfere with the other term, but this interference is not enough to mask the mainlobe of the other term. Likewise the third term of Eq. (3.4) interferes with the other two terms, but is not large enough to mask the locations of the maximums. (The only time this term becomes significant is when ω^v and ω^r are such that the mainlobes of the individual factors coincide. The only case for which this occurs is at $\omega^v = \omega^r = 0$, and in this case it serves to reinforce the other two terms of Eq. (3.4). So ω^v and ω^r can be determined from either of these maximums.

3.2 One-Dimensional Method

An alternative method of retrieving range and velocity information is to treat the two-dimensional array x(n,m) as a one-dimensional sequence $x(\ell)$ and then take the magnitude squared of the DFT of the sequence $x(\ell)$. The sequence $x(\ell)$ and the array x(n,m) can be related as follows:

$$x(n,m) \xrightarrow{\quad \ell = nM + m \quad} x(\ell)$$

$$0 \leq n \leq N-1 \qquad\qquad 0 \leq \ell \leq NM-1$$

$$0 \leq m \leq M-1$$

or

$$x(\ell) \xrightarrow[m = \ell - M\langle\frac{\ell}{M}\rangle]{n = \langle\frac{\ell}{M}\rangle} x(n,m)$$

$$0 \leqslant \ell \leqslant NM-1 \qquad\qquad 0 \leqslant n \leqslant N-1$$

$$0 \leqslant m \leqslant M-1$$

where the notation $\langle\ \rangle$ implies that the enclosed argument should be truncated to an integer.

In practice the sequence $x(\ell)$ is obtained directly from sampling the radar signal without reordering. The samples are, however, labeled sequentially in terms of ℓ instead of n and m.

For the case of one discrete target the sequence $x(\ell)$ can be expressed mathematically as follows:

$$x(\ell) = \cos 2\pi \left(\ell - M\langle\frac{\ell}{M}\rangle\omega^r + \langle\frac{\ell}{M}\rangle\omega^v + \phi \right)$$

$$0 \leqslant \ell \leqslant NM - 1 \ .$$

By definition the DFT of the sequence $x(\ell)$ is

$$X(k) = \frac{1}{NM} \sum_{\ell=0}^{NM-1} x(\ell) e^{-j2\pi\ell k/NM} \ . \tag{3.5}$$

Physically, performing this DFT is straightforward. But because of the nature of the radar signal, to evaluate this analytically it is convenient to express the signal as $x(n,m)$ rather than $x(\ell)$. And since $\ell = nM + m$, the above expression for the DFT is mathematically equivalent to the following:

$$X(k) = \frac{1}{NM} \sum_{n=0}^{N-1} \sum_{m=0}^{M-1} x(n,m) e^{-j2\pi(nM+m)k/NM} \ . \tag{3.6}$$

Substituting in $x(n,m)$ as defined in Eq. (3.1) gives

$$X(k) = \frac{1}{NM} \sum_{n=0}^{N-1} \sum_{m=0}^{M-1} \cos 2\pi(m\omega^r + n\omega^v + \phi) e^{-j2\pi(nM+m)k/MN} \ . \tag{3.7}$$

Then evaluating the right-hand side and taking the magnitude square gives

$$|X(k)|^2 = \frac{1}{4}\frac{1}{(NM)^2}\left[\frac{\sin N\pi(\omega^v - k/N)\ \sin M\pi(\omega^r - k/NM)}{\sin\pi(\omega^v - k/N)\ \sin\pi(\omega^r - k/NM)}\right]^2$$

$$+ \frac{1}{4}\frac{1}{(NM)^2}\left[\frac{\sin N\pi(\omega^v + k/N)\ \sin M\pi(\omega^r + k/NM)}{\sin\pi(\omega^v + k/N)\ \sin\pi(\omega^r + k/NM)}\right]^2 \qquad (3.8)$$

$$+ \frac{1}{2}\frac{1}{(NM)^2}\left\{\frac{\sin N\pi(\omega^v - k/N)\ \sin N\pi(\omega^v + k/N)\ \sin M\pi(\omega^r - k/NM)\ \sin M\pi(\omega^r + k/NM)}{\sin\pi(\omega^v - k/N)\ \sin\pi(\omega^v + k/N)\ \sin\pi(\omega^r - k/NM)\ \sin\pi(\omega^r + k/NM)}\right.$$

$$\left.\times \cos 2\pi[\omega^v(N-1) + \omega^r(M-1) + 2\phi]\right\} .$$

This is the power spectrum of the sequence $x(\ell)$. It can be seen that ω^v and ω^r determine the locations of the maximums.

For a better understanding of the interpretation of this spectrum, consider the first term of Eq. (3.8):

$$\left[\frac{\sin N\pi(\omega^v - k/N)\ \sin M\pi(\omega^r - k/NM)}{\sin\pi(\omega^v - k/N)\ \sin\pi(\omega^r - k/NM)}\right]^2 . \qquad (3.8a)$$

It is the product of two functions. The function

$$\left[\frac{\sin N\pi(\omega^v - k/N)}{\sin\pi(\omega^v - k/N)}\right]^2$$

repeats itself every N samples. The value of ω^v determines the locations of the maximums. If $\omega^v = 0$ (therefore velocity = 0), the maximums will occur at $k = 0$, $k = \pm N, \pm 2N, \ldots \pm jN$ where j is an integer; if the target is moving ($\omega^v \neq 0$), the function will be shifted away from the zero velocity position by the amount $\Delta k = \omega^v N$ (Fig. 3.3). To prevent aliasing, $|\omega^v| < 0.5$, and therefore $|\Delta k| < N/2$. Because of this, any section of N points along the k axis can be used to determine the velocity spectrum. It is most convenient to view a section where

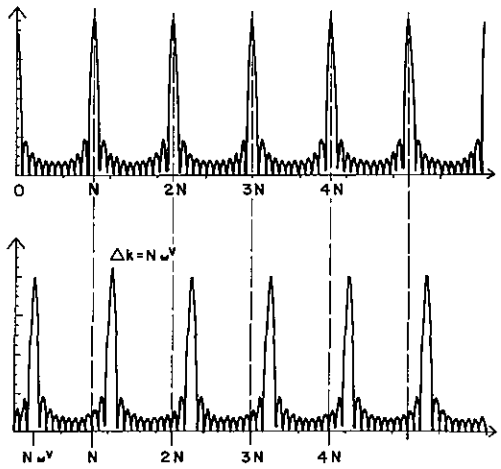

Figure 3.3.--Velocity spectrum for a stationary target (above) and for a moving target (below). For a stationary target, the maximums occur at integer multiples of N. For a moving target, the maximums are shifted from their zero velocity position by the amount $\Delta k = N\omega^{v}$.

$$jN - \frac{N}{2} \leqslant k \leqslant jN + \frac{N}{2}$$

and j is an integer (Fig. 3.4). Then jN corresponds to the zero velocity point: If the maximum shifts to the left it corresponds to negative velocities; if it shifts to the right it corresponds to positive velocities. A section like this is referred to as a "range cell."

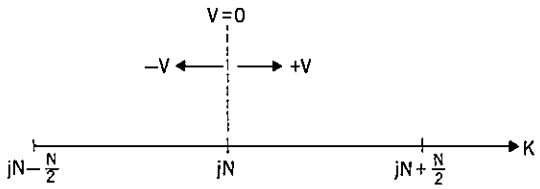

Figure 3.4.--A diagram of the jth range cell, the center of which is k = jN and corresponds to the zero velocity point. To the right is positive velocity; to the left is negative velocity.

The function

$$\left| \frac{\sin M\pi(\omega^{r} - k/NM)}{\sin \pi(\omega^{r} - k/NM)} \right|$$

is shown in Fig. 3.5 for $\omega^{r} = 0$. For $\omega^{r} \neq 0$ the function shifts by an amount $\Delta k = \omega^{r}$ MN. When multiplied by the function

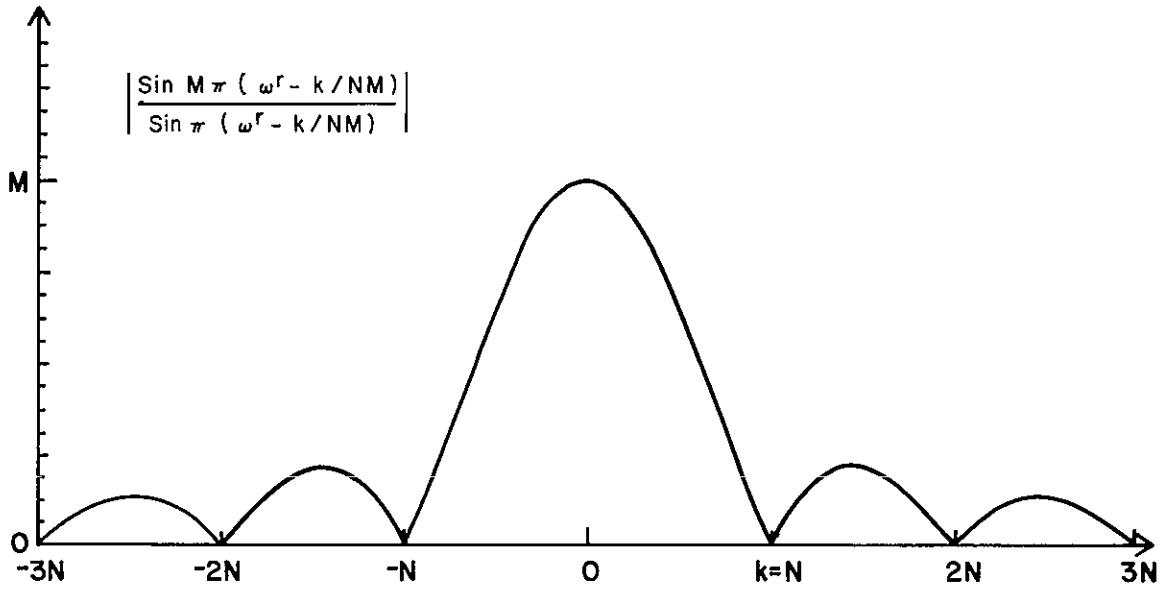

Figure 3.5.--A section of the $|\sin M\pi(\omega^r - k/NM)/\sin\pi(\omega^r - k/NM)|$ function. In this case $\omega^r = 0$; therefore, the mainlobe is centered at $k = 0$.

$$\frac{\sin N\pi(\omega^v - k/N)}{\sin\pi(\omega^v - k/N)}$$

its broad mainlobe will "select" a "range cell" and its associated portion of the velocity spectrum. Outside this range cell, selected by the mainlobe, the velocity spectra will be attenuated because they are multiplied by the sidelobes of the range spectrum. Figure 3.6 illustrates the retrieval of ω^r and ω^v from the spectrum.

The second term in Eq. (3.8),

$$\left[\frac{\sin N\pi(\omega^v + k/N)\ \sin M\pi(\omega^r + k/NM)}{\sin\pi(\omega^v + k/N)\ \sin\pi(\omega^r + k/NM)}\right]^2 , \qquad (3.8b)$$

is identical to (3.8a) except that it shifts in the opposite direction in response to ω^v and ω^r. The mainlobe of this term overlaps with the mainlobe of the previously discussed term only when the target is located in the range cell centered at $k = 0$. For this reason it is not possible to distinguish positive from negative velocities in the first range cell. (This same effect also occurs in the last range cell, which is centered at $k = NM/2$ and corresponds to the "foldover" frequency.)

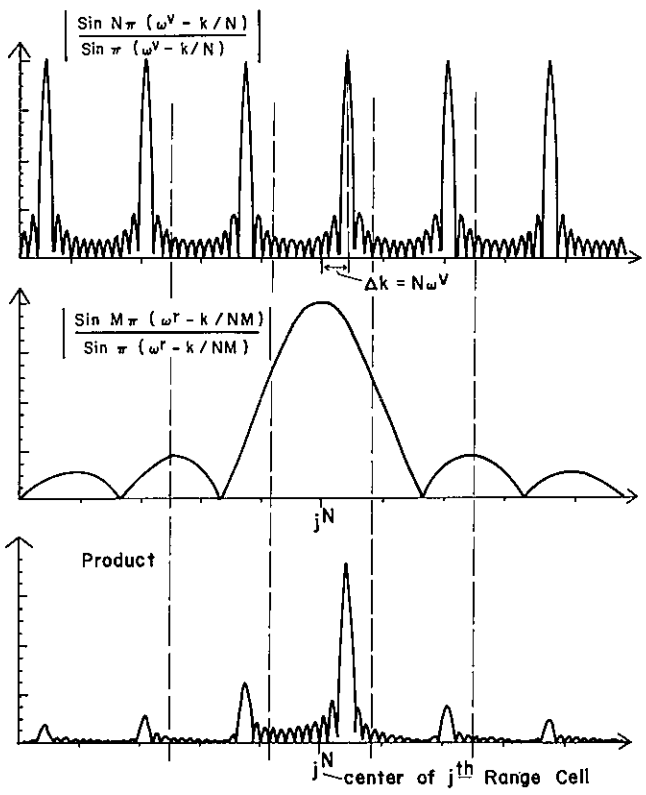

Figure 3.6.--(Top) The velocity spectrum; each mainlobe is displaced an amount $\Delta k = Nw^v$ from the center of a range cell. (Middle) The function $|\sin M\pi(\omega^r - k/NM)/\sin\pi(\omega^r - k/NM)|$; ω^r is such that the center of the mainlobe is in the center of the jth range cell. (Bottom) The product of the two.

The third term of the equation is

$$\frac{\sin N\pi(\omega^v - k/N)\ \sin N\pi(\omega^v + k/N)\ \sin M\pi(\omega^r - k/NM)\ \sin M\pi(\omega^r + k/NM)}{\sin\pi(\omega^v - k/N)\ \sin\pi(\omega^v + k/N)\ \sin\pi(\omega^r - k/NM)\ \sin\pi(\omega^r + k/NM)}$$

$$\times \cos 2\pi[\omega^v(N-1) + \omega^r(M-1) + 2\phi] \quad . \tag{3.8c}$$

It can be seen that this term will interfere with the other terms of the spectrum, but it does not get large enough to mask the critical parts of the spectrum except when $\omega^v = 0$, $\omega^r = 0$; when this occurs it interferes constructively.

One final remark about the spectrum described by Eq. (3.8): It is symmetrical about $k = 0$, and periodic every $k = MN$. Therefore, when the spectrum is analyzed, it is necessary to consider only $0 \leqslant k \leqslant MN/2$.

4. RANGE SPREADING

Ideally, the spectrum due to one discrete target would be composed of delta functions, but due to the fact that the DFT's are of finite length the spectrum contains the sinNx/sinx functions instead of the delta functions. This is true regardless of which processing method is used. The undesirable effect is that the sidelobes of the range spectrum allow the velocity spectrum to exist in range cells other than the correct one. This effect is referred to as range spreading.

The most obvious effect of range spreading is the illusion that targets exist where, in reality, they do not. For the case of one target this would not be a problem. Because the sidelobes are approximately 13 dB or more below the mainlobe it would be apparent which range cell was the correct one. The case of just one target is, however, the idealized case. In general, the radar will be detecting more than one target, and the power spectrum will be the superposition of the spectrum due to each target. Therefore it is not possible simply to attribute the strongest spectral component to a real target and the weaker spectral components to the sidelobe structure of the spectrum due to that target. These weaker spectral components could be due to targets of smaller radar cross section relative to a target with stronger return.

When the radar is used to study the atmosphere (or other distributed target), radar return may be expected for many range cells. And each of these range cells is expected to have an associated velocity spectrum representing a distribution of velocities. In cases such as this, knowledge of the shape of the velocity spectrum is important. It is therefore undesirable for energy associated with a given range to interfere with the velocity spectra associated with other ranges. As a result, the shape of the velocity spectrum may be altered, or in extreme cases completely lost.

4.1 Two-Dimensional Case

The effects of range spreading differ, depending on which processing method is used. The two-dimensional (2-D) case is fairly straightforward. One sample of the range spectrum will weight the entire velocity spectrum for a given range cell. The worst case occurs when samples of the range spectrum are taken at the maximums of the sidelobes. In such a case, the maximum possible value is weighting the velocity spectrum in the undesired range cells. The best case occurs when the samples of the range spectrum are taken at the nulls of the sinNx/sinx term and at the center of the mainlobe. In such a case the sample at the center of the mainlobe weights the desired range cell while all the other range cells are weighted with zero (see Fig 4.1).

The sampling points of the range spectrum are fixed by the definition of the DFT. The degree of range spreading is determined by the value of ω^r. If the value of ω^r is such that the mainlobe of the range spectrum coincides with a sampling point, then range spreading is minimized. Mathematically, this occurs when

$$\omega^r = \frac{k}{M} \qquad k = \text{integer} \ . \tag{4.1}$$

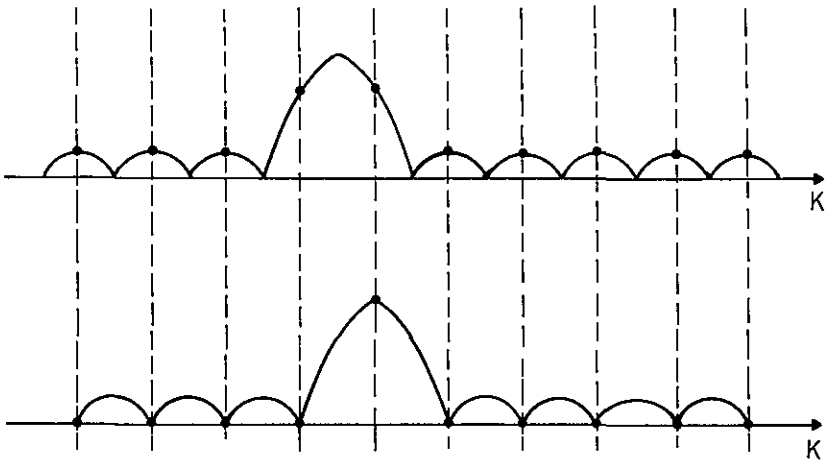

Figure 4.1.--Two cases illustrating that the amount of range spreading is a function of ω^r. In both cases $\sin M\pi(\omega^r - k/M)/\sin\pi(\omega^r - k/M)$ is plotted as a function of k. Samples of this function weight the velocity spectra of different range cells. The sampling points are fixed by the DFT. They occur at integer values of k. So the value of ω^r determines where this curve will be sampled. The top plot illustrates the worst case when ω^r is such that the mainlobe falls exactly between sampling points (represented by broken lines). The bottom figure illustrates the best case when $M\omega^r$ is an integer value, so that the center of the mainlobe coincides with a sampling point.

Substituting for ω^r and rearranging to express k in terms of range, velocity, and radar parameters, gives

$$k = \frac{2MB}{f_s Tc}\left[R_o + (f_o \frac{T}{B})v\right]. \qquad (4.2)$$

This equation expresses how bad range spreading of a target will be for a specific range and velocity. The farther k is from being an integer, the worse the range spreading. The equation will be used later to find ranges and velocities for some examples of worst case and best case range spreading.

4.2 One-Dimensional Case

In the one-dimensional (1-D) case, each sample of the velocity spectrum is weighted by a different sample of the range spectrum, as is apparent from Eq. (3.8). (This is the main difference relative to the 2-D method, where the N samples of the velocity spectrum corresponding to a range cell were all weighted by the same sample of the range spectrum.) It has been shown that the velocity spectrum repeats itself every N samples, and that the range spectrum (which repeats every NM samples) weights the velocity spectrum (Fig. 3.6). The mainlobe of the range spectrum "selects" a range cell and its associated velocity spectrum; it is left to the sidelobe structure of the range spectrum to suppress the velocity spectrum in the other range cells. Of course the suppression of the velocity spectrum in range cells other than the correct one is not complete. Therefore the velocity spectrum, although attenuated, appears in range cells other than the correct one, and this is referred to as range spreading.

The degree of range spreading is determined by the relative values of ω^r and ω^v, which determine the amount the range spectrum and the velocity spectrum, respectively, have shifted from zero. The relative positioning of the two spectra determines how the velocity spectrum will be weighted by the range spectrum. In the ideal case (Fig. 4.2), the nulls of the range spectrum are positioned relative to the velocity spectrum where they would contribute the most to suppressing range spreading when the two terms are multiplied together. That is, the nulls of the range spectrum coincide with the center of the velocity spectrum in range cells other than the correct one. The worst case occurs (Fig. 4.3) when the centers of the sidelobes on the range spectrum coincide with these critical points of the velocity spectrum.

It is possible to express mathematically how bad range spreading will be for a target at a given velocity and range. This can be approached from the time domain or frequency domain. When the approach is from the frequency domain, the center of the mainlobe of the range spectrum is located at

$$k = MN\omega^r \quad . \tag{4.3}$$

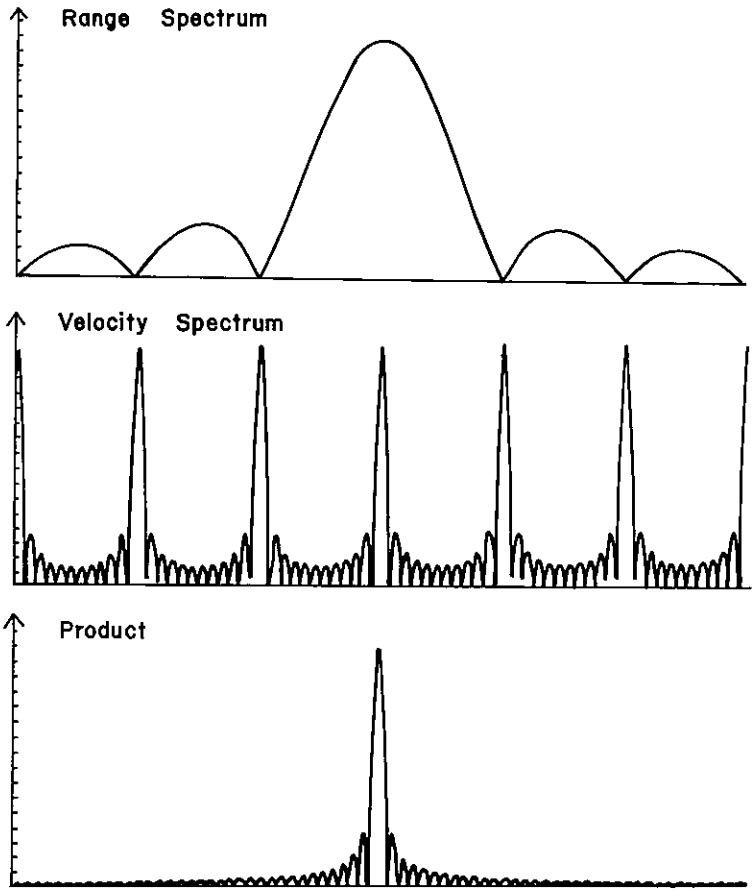

Figure 4.2.--The conditions that minimize range spreading when the 1-D method of processing is used: (Top) the range spectrum; (Middle) the velocity spectrum; (Bottom) the product of the two.

The velocity spectrum has a maximum every N points, so its maxima are located at

$$k = jN + N\omega^v \tag{4.4}$$

where j is an integer. The condition for minimum range spreading is for the maximum of the range spectrum to coincide with a maximum of the velocity spectrum, or

$$MN\omega^r = jN + N\omega^v \tag{4.5}$$

or

$$j = M\omega^r - \omega^v \ .$$

When j is an integer, range spreading is minimum. The farther j is from being an integer, the worse the range spreading will be.

Substituting for ω^r and ω^v to express this relationship in terms of range, velocity, and radar parameters we obtain

$$j = \frac{2MB}{f_s Tc} R - \frac{T}{B} f_o \left(\frac{f_s}{M} G - 1\right) v \ . \tag{4.6}$$

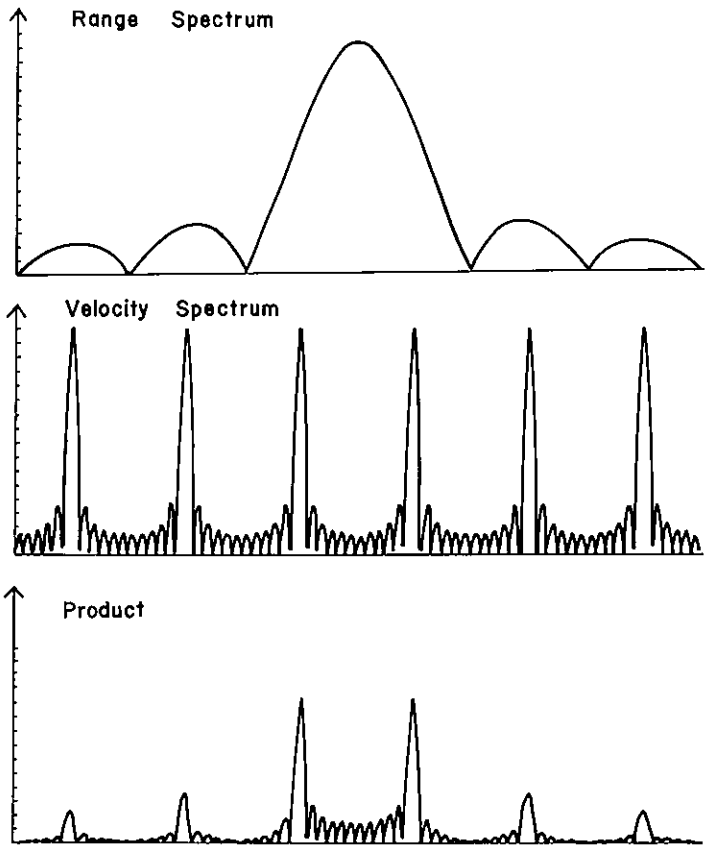

Figure 4.3.--The conditions resulting in worst case range spreading: (Top) the range spectrum; (Middle) the velocity spectrum; (Bottom) the product of the two.

Alternatively, a time domain approach can be used to derive the above, the idea being that if discontinuities in the time series did not exist between sweeps, the spectrum would be "better."

The signal during the nth sweep can be written as

$$\cos 2\pi(m\omega^r + \phi_n)$$

where $\phi_n = n\omega^v + \phi$

and, during the next sweep, as

$$\cos 2\pi(m\omega^r + \phi_{n+1})$$

where $\phi_{n+1} = (n+1)\omega^v + \phi$.

Because the first sample (m = 0) at the n + 1 sweep immediately follows the last sample (m = M - 1) of the nth sweep, the following is sufficient to eliminate the discontinuity:

$$(m\omega^r + \phi_n)\Big|_{m=M} = (m\omega^r + \phi_{n+1} + j)\Big|_{m=0} \qquad (4.7)$$

where j is an integer, inserted because multiplication by an integer will just increase the phase by an integer multiple of 2π. So

$$M\omega^r = \omega^v + j,$$

which is the same as the result obtained from the previous approach.

4.3 Other Considerations

When the spectrum is interpreted, some other effects besides range spreading may have to be taken into consideration. Recall that the spectrum for one target is the sum of three terms (Eq. 3.4 or Eq. 3.8). Although just one of these terms is of interest, the other two terms contribute to the spectrum in the form of interference. These terms will contribute energy to incorrect range cells, thereby reinforcing the effects of range spreading. And the energy they add to the correct range cell will bias the velocity spectrum to some extent.

In the 1-D case it must be remembered that a different point of the range spectrum weights each point of the velocity spectrum. Therefore, the velocity spectrum is weighted unevenly across the range cell. This will cause some distortion in the velocity spectrum, especially in the case of a wideband velocity spectrum. A simple example is shown below (one range cell is illustrated). Another situation to be aware of occurs when the mainlobe of the range spectrum is between two range cells (as in Fig. 4.3). This is the case of maximum range spreading, but there is another effect. The velocity

spectrum is "shared" between two range cells. This is expected, especially when a target is located at a range halfway between two range cells. Calculation of the total power to be associated with a target must take this effect into account.

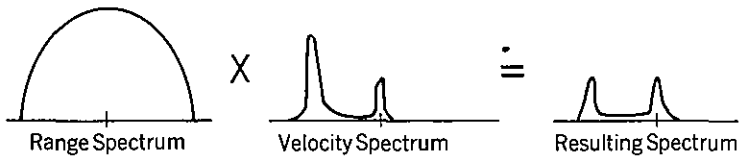

In the 2-D case the velocity spectrum in a range cell is weighted by one sample of the range spectrum, so the problem of the spectrum's being unevenly weighted across the range cell does not exist. But the sample weighting the velocity spectrum may not be at the maximum of the mainlobe of the range spectrum, so the actual energy to be associated with the velocity spectrum may be more than it seems to be. If the weighting sample is far enough from the center of the mainlobe, the adjacent range cell will also be weighted by a significant sample from the mainlobe. In this case the total energy to be associated with the target can be approximated by considering both range cells. Once again, a target is "shared" between two range cells when significant range spreading is occurring elsewhere in the spectrum. Therefore, whether 1-D processing or 2-D processing is used, the degree that a target is "split" between two range cells is a good indication as to how much this target will bias the spectrum of another target through range spreading.

5. WINDOWING TO REDUCE RANGE SPREADING

5.1 The Windowing Method

The range spreading effect is very undesirable. As noted, it is a result of the sidelobe structure of the spectrum due to finite data length. This is a very common problem. A standard method of dealing with it applies a window to weight the data multiplicatively. This reduces discontinuities in the data and thereby reduces the sidelobe in the frequency domain.

In general, windows are easy to implement. (Multiply incoming data by samples of the window.) Different windows have certain advantages and disadvantages. The most important characteristic is the relationship between mainlobe width and sidelobe level. There is an unavoidable tradeoff between the two; in order to obtain lower sidelobe levels one must be willing to accept a broader mainlobe. (Sidelobe level and mainlobe width as well as other figures of merit for many of the most common windows are given in Harris, 1978.)

To reduce the sidelobe levels on the range spectrum the window must be applied to each sweep of data individually. In this way the data (and some derivatives) will be forced to zero at the discontinuities. Of course, broadening of the mainlobe results, and this has some undesirable effects. The effective width of the mainlobe can increase by a factor of 2 or even more, depending on the window used. It will encompass a great deal more than just

one range cell. Two adjacent range cells could fall between the 6-dB points of the mainlobe. A velocity spectrum originally contained in one range cell would then dominate the adjacent range cell to a large extent, thereby decreasing the effective range resolution. This is illustrated in Fig. 5.1. This effect is unacceptable when it is critical to be able to compare the velocity spectra from adjacent range cells, as in measurement of wind shear.

To test the effects of windowing, a computer model of the radar was used to generate data. A few of the more promising windows were considered, and results follow.

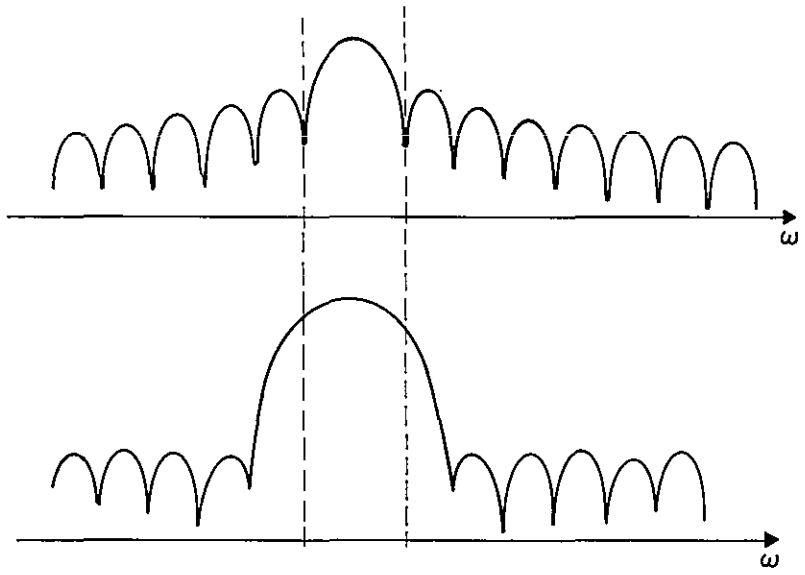

Figure 5.1.--Mainlobe width of the range spectrum (above) before and (below) after windowing with a typical window, such as the Hamming window.

5.2 Windowing Simulated Radar Data

Essentially, Eq. (2.7) was used to generate radar data. Windowing and spectrum analysis (by use of the DFT) could then be done on this simulated data. The radar parameters used in this study are given in Table 5.1.

The cases selected to test windowing were the "worst case" range spreading and the "best case" range spreading for both the 2-D and 1-D methods. The ranges and velocities necessary to give these ideal cases were calculated from (4.6) and (4.2).

5.2.1 Format of Plots

Regardless of the processing method used (1-D or 2-D) to obtain the spectrum, the spectrum will be plotted as indicated in the following figure, to yield range and velocity information.

Table 5.1.--Radar parameters used in computer simulation

Parameter	Value
f_o	3.0×10^9 Hz
B	5.0×10^6 Hz
T	2.778×10^{-3} s
G	2.778×10^{-3} s
c	3.0×10^8 m/s
f_s	48,000 Hz
M	32
N	32
Range resolution	125 meters
Maximum unambiguous range	2000 meters
Velocity resolution	0.56 m/s
Unambiguous velocity	$-8.44 < v < 8.44$ m/s

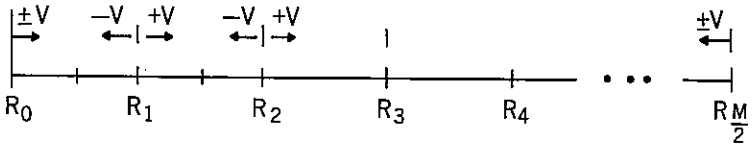

R_m defines the center (and therefore zero velocity point) of the mth range cells. Moving to the right of center corresponds to positive velocity, to the left, negative velocity. A range cell contains N samples of the velocity spectrum, and there are M/2 range cells. Each of the N samples of the velocity spectrum corresponds to an incremental change in velocity, which is labled VRES on the graphs. Likewise, R RES defines the incremental change in range from one range cell to the next.

When the 1-D method is used for processing, the above format is obtained simply by plotting the power spectrum for $0 < \Omega < \pi$, where Ω is the normalized frequency variable $\Omega = 2\pi\ k/NM$. When the 2-D method is used, the 2-D spectrum has to be rearranged slightly to appear in this format.

5.2.2 Results

Figures 5.2 through 5.5 show the spectra for four cases (1-D best and worst, and 2-D best and worst), unmodified and modified by five different windows. It can be seen that when a window is applied to the "best case" condition the spectrum gets "worse." This is expected, since in the "best case" the nulls of the range spectrum weight the velocity spectrum in the undesired range cells (before windowing). After windowing, the range spectrum still has nulls but these have been shifted because most windows have their nulls in different places compared with the rectangular window. This effect must be kept in mind when comparing the effects of windowing on the spectra.

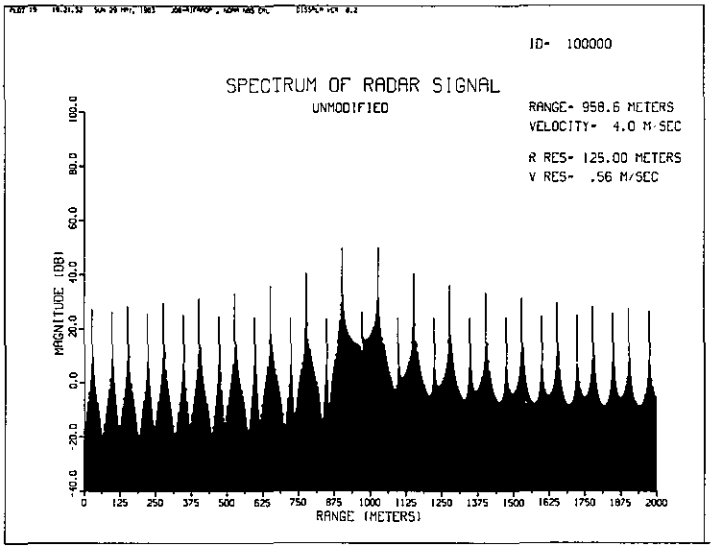

Figure 5.2.--Effect of windowing on spectrum of radar signal for 1-D worst case. Range is 958.6 m; velocity is 4.0 m/s.

Figure 5.2a.--Unmodified.

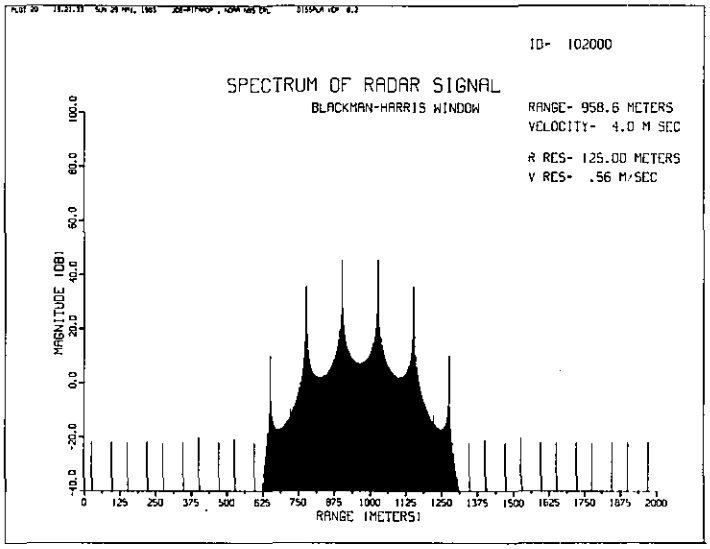

Figure 5.2b.--Blackman-Harris window.

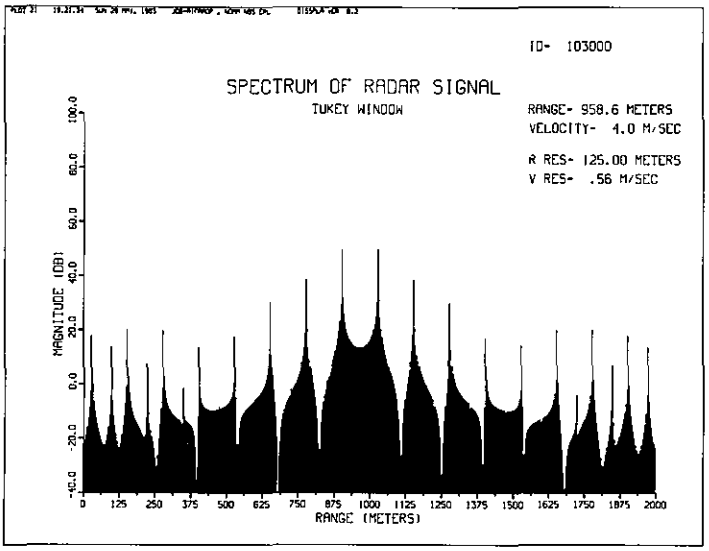

Figure 5.2c.--Tukey window.

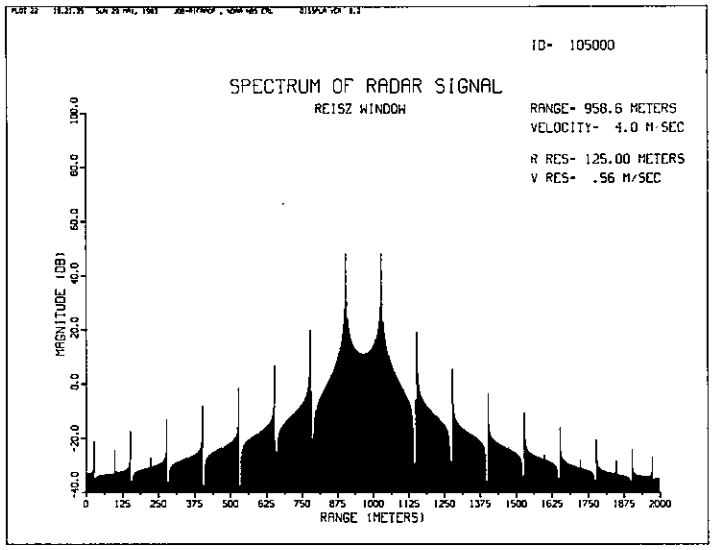

Figure 5.2d.--Riesz window.

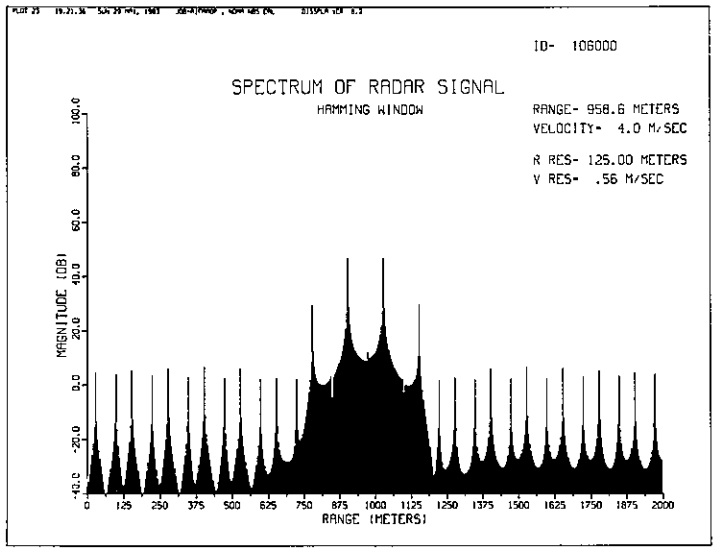

Figure 5.2e.--Hamming window.

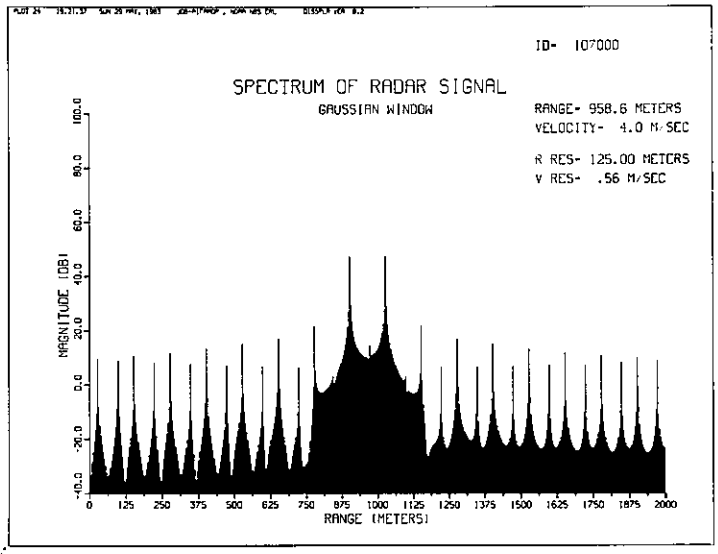

Figure 5.2f.--Gaussian window.

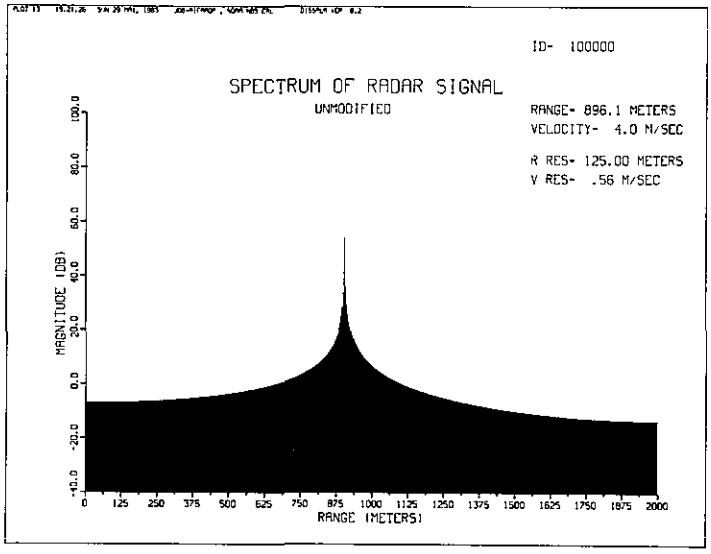

Figure 5.3.--Effect of windowing on spectrum of radar signal for 1-D best case. Range is 896.1 m. Velocity is 4.0 m/s.

Figure 5.3a.--Unmodified.

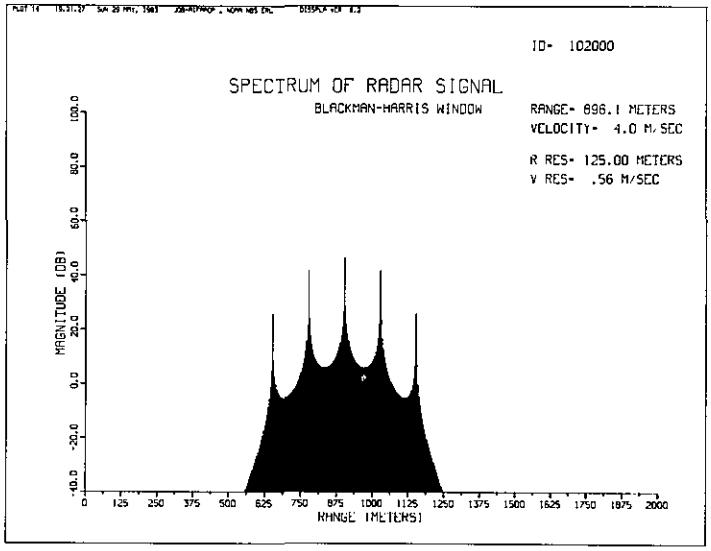

Figure 5.3b.--Blackman-Harris window.

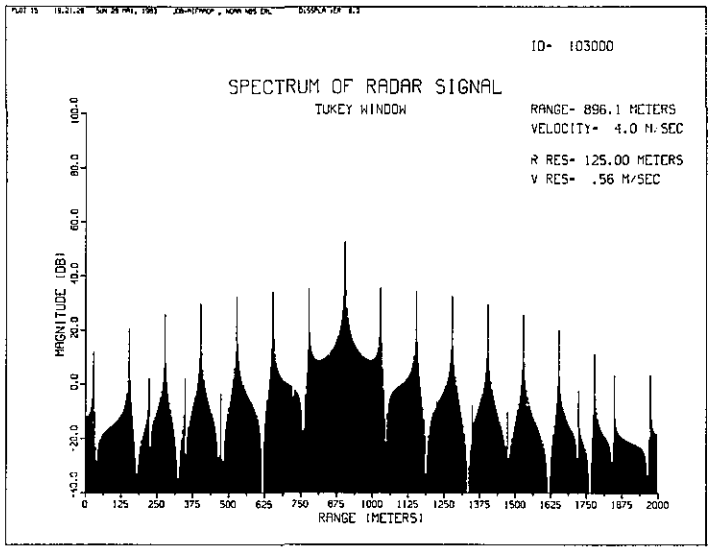

Figure 5.3c.--Tukey window.

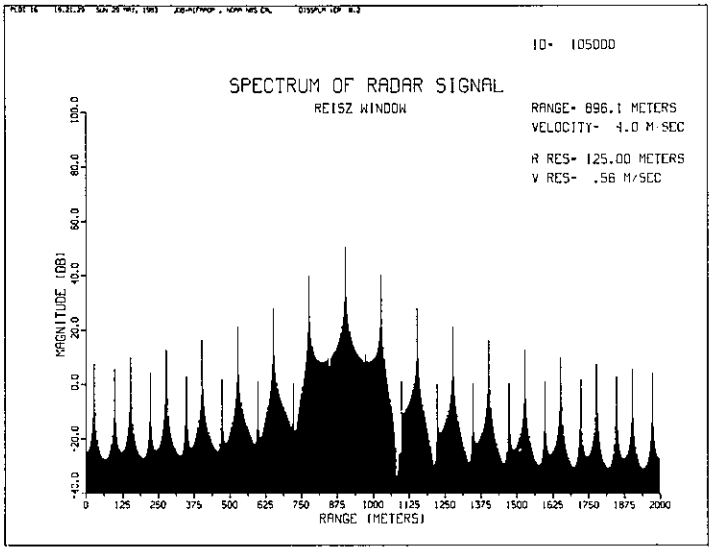

Figure 5.3d.--Riesz window.

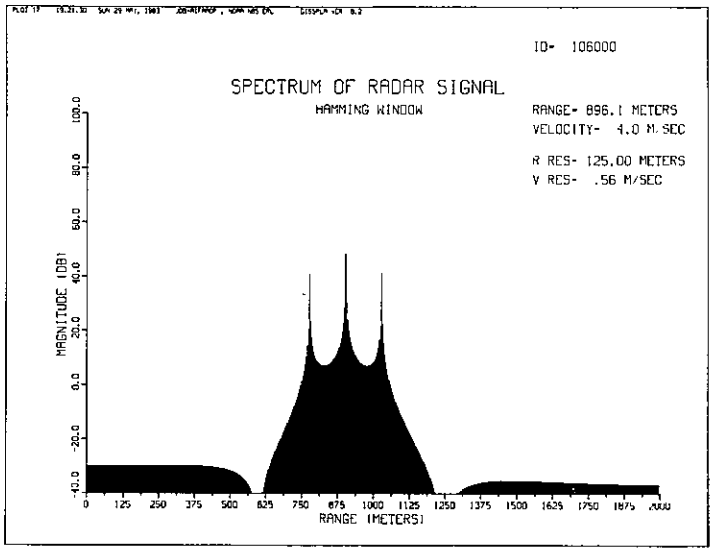

Figure 5.3e.--Hamming window.

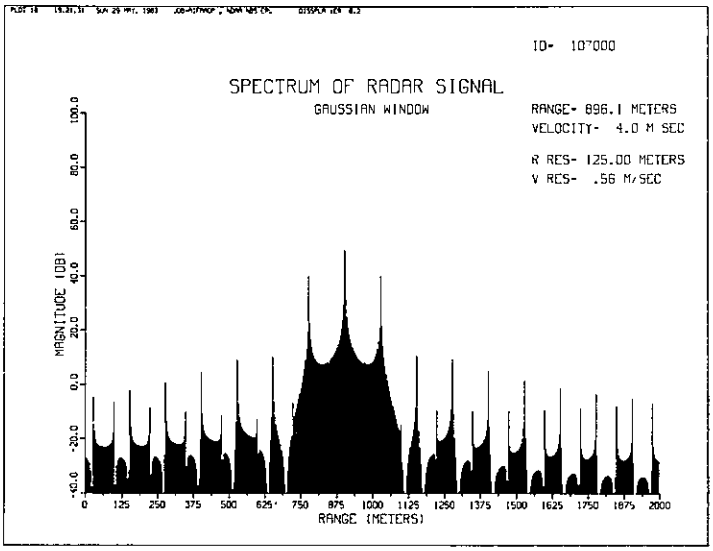

Figure 5.3f.--Gaussian window.

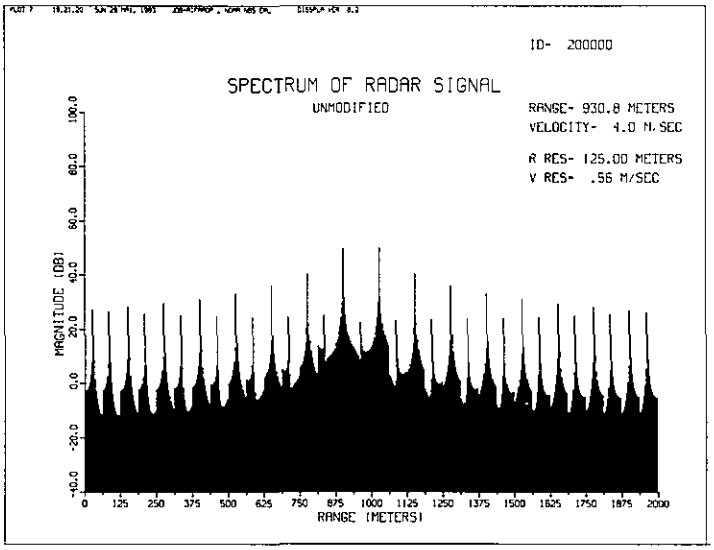

Figure 5.4.--Effect of windowing on spectrum of radar signal for 2-D best case. Range is 930.8 m. Velocity is 4.0 m/s.

Figure 5.4a.--Unmodified.

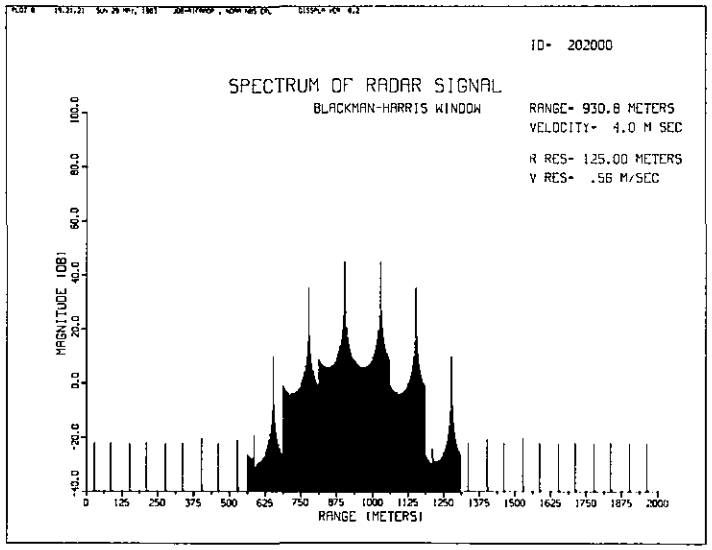

Figure 5.4b.--Blackman-Harris window.

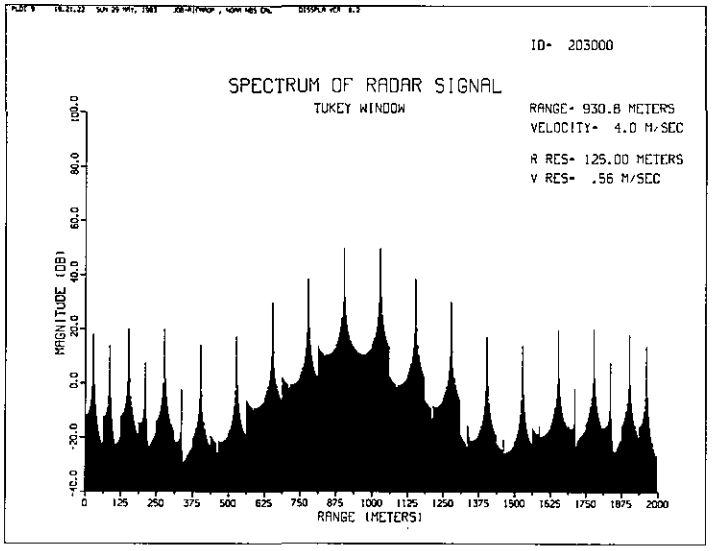

Figure 5.4c.--Tukey window.

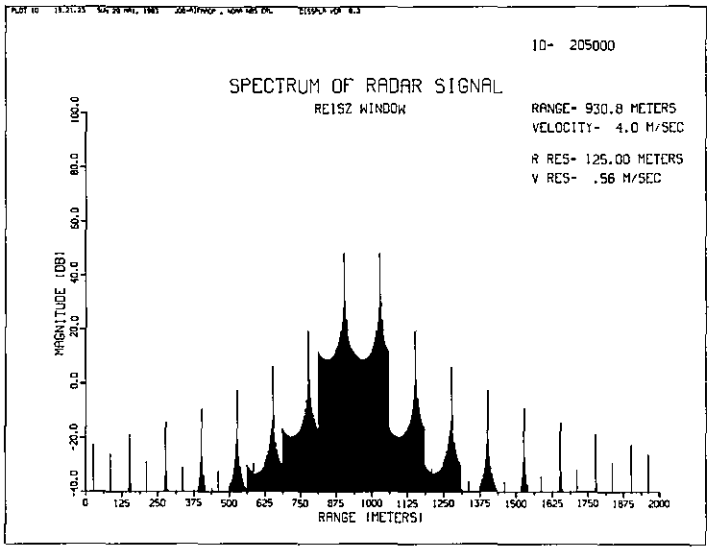

Figure 5.4d.--Riesz window.

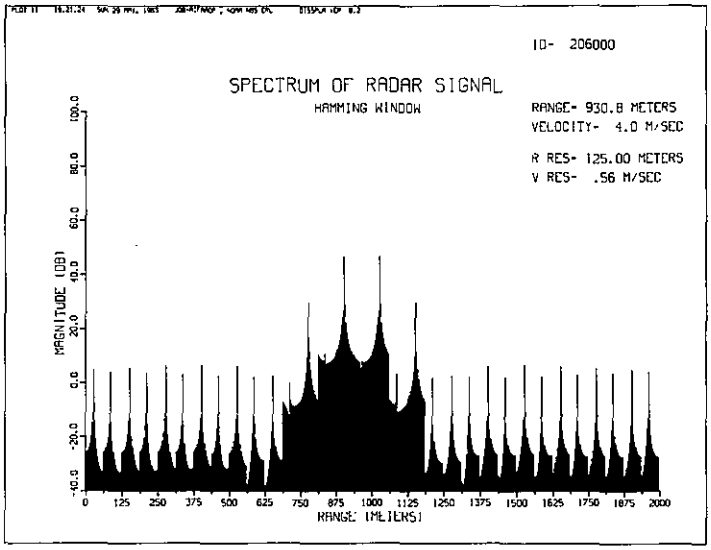

Figure 5.4e.--Hamming window.

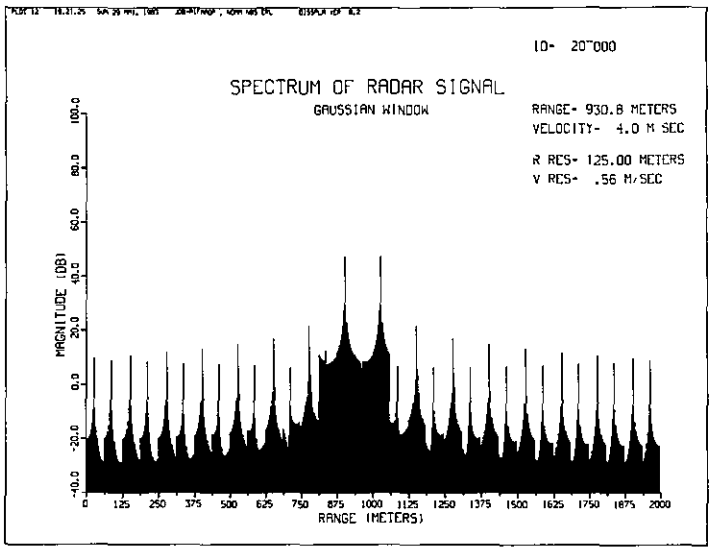

Figure 5.4f.--Gaussian window.

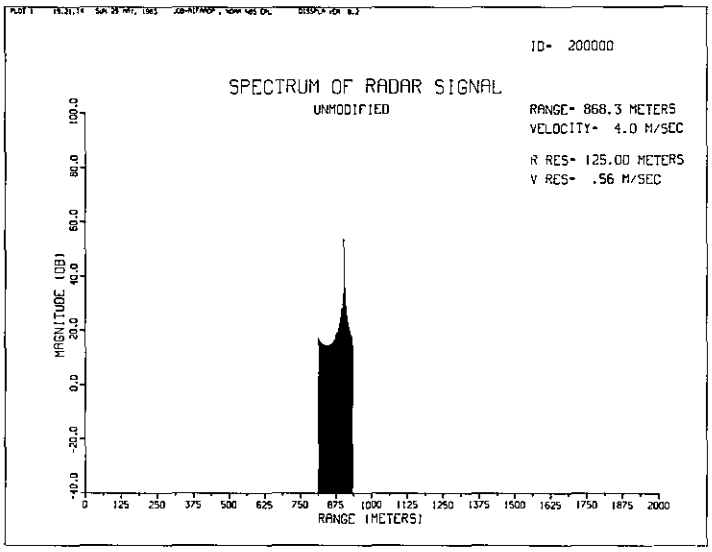

Figure 5.5.--Effect of windowing on spectrum of radar signal for 2-D best case. Range is 868.3 m. Velocity is 4.0 m/s.

Figure 5.5a.--Unmodified.

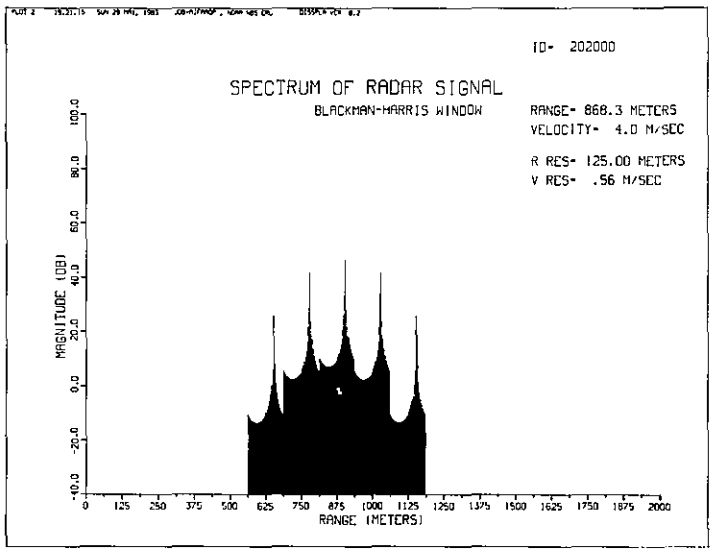

Figure 5.5b.--Blackman-Harris window.

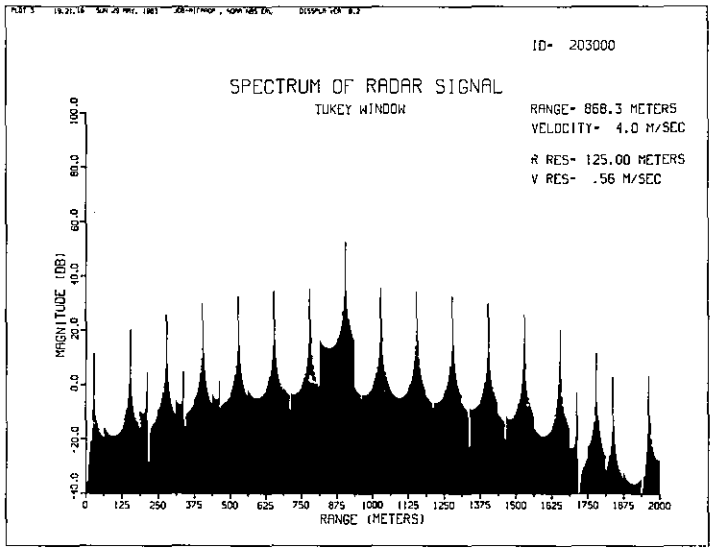

Figure 5.5c.--Tukey window.

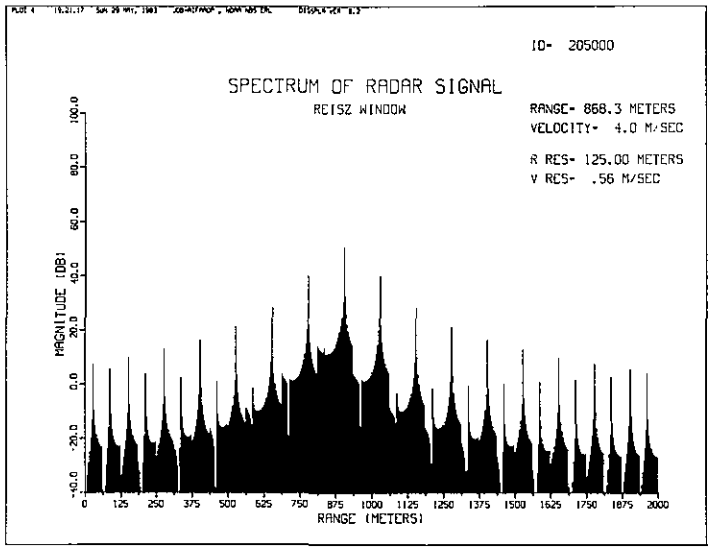

Figure 5.5d.--Riesz window.

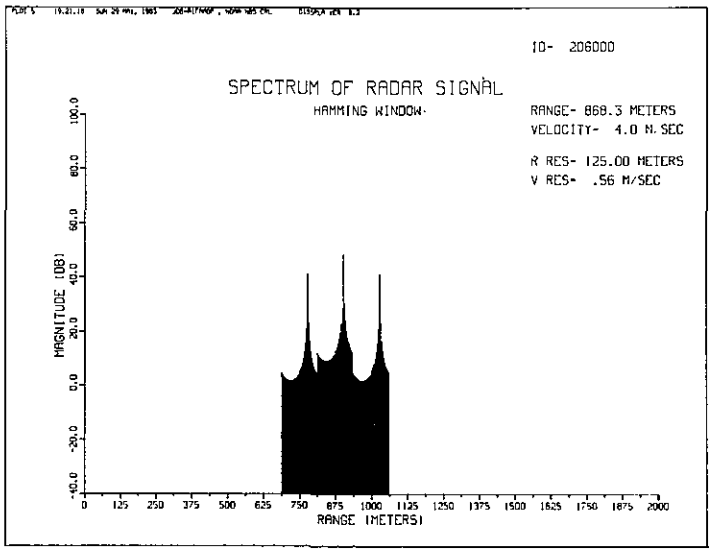

Figure 5.5e.--Hamming window.

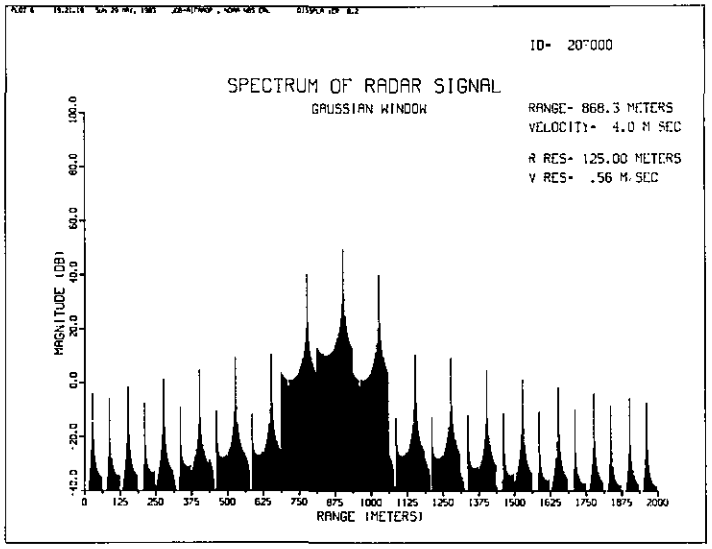

Figure 5.5f.--Gaussian window.

6. AD HOC METHODS OF SMOOTHING

When the 1-D method is used to process the data, the return from each radar sweep is placed immediately after the return from the previous sweep. The result is one sequence of data of length MN. There are, in general, rough discontinuities in the data where one sweep ends and the next begins. The more drastic the discontinuity the more pronounced the range spreading will be. Several ad hoc methods may be used to smooth the data of the discontinuity in the hope of reducing the amount of range spreading.

6.1 Three-Point Average of Two Points

With this method the first point of each sweep is replaced by the average value of itself combined with its two adjacent points. Likewise, the last point of each sweep is replaced by the average value of itself and its two adjacent points.

That is,

$$\hat{x}(n,1) = \frac{1}{3}\,[x(n-1,M) + x(n,1) + x(n,2)]$$

$$\hat{x}(n,M) = \frac{1}{3}\,[x(n,M-1) + x(n,M) + x(n+1,1)]$$

where $\hat{x}(n,M)$ is the calculated value to replace $x(n,M)$.

Also in calculating the replacement value of the first point of the first sweep and the last point of the last sweep, the sequence is treated as though it were cyclic; that is, the first sweep follows the last. So

$$\hat{x}(1,1) = \frac{1}{3}\,[x(N,M) + x(1,1) + x(1,2)]$$

$$\hat{x}(N,M) = \frac{1}{3}\,[x(N,M-1) + x(N,M) + x(1,1)]\ .$$

6.2 Five-Point Average of Two Points

With this method the first point of each sweep is replaced by the average value of itself and its four surrounding points. Likewise the last point of each sweep is replaced by the average value of itself and its four surrounding points. That is,

$$\hat{x}(n,1) = \frac{1}{5}\,[x(n-1,M-1) + x(n-1,M) + x(n,1) + x(n,2) + x(n,3)]$$

$$\hat{x}(n,M) = \frac{1}{5}\,[x(n,M-2) + x(n,M-1) + x(n,M) + x(n+1,1) + x(n+1,2)]$$

where $\hat{x}(n,m)$ is the calculated value that is to replace $x(n,m)$.

Once again the sequence is assumed to be cyclic when we calculate the replacement value for the first point of the first sweep and the last point of the last sweep.

6.3 Three-Point Average of Four Points

This method replaces the first two points and the last two points of each sweep with a three-point average. The three-point average is found by considering the point to be replaced and its two adjacent points and finding the average of these three points. That is,

$$\hat{x}(n,1) = \frac{1}{3}\,[x(n-1,M) + x(n,1) + x(n,2)]$$

$$\hat{x}(n,2) = \frac{1}{3}\,[x(n,1) + x(n,2) + x(n,3)]$$

$$\hat{x}(n,M-1) = \frac{1}{3}\,[x(n,M-2) + x(n,M-1) + x(n,M)]$$

$$\hat{x}(n,M) = \frac{1}{3}\,[x(n,M-1) + x(n,M) + x(n+1,1)]\ .$$

Once again the sequence is assumed to be cyclic when the replacement values for the first two points of the first sweep and the last two points of the last sweep are calculated.

6.4 Five-Point Average of Four Points

This method replaces the first two points and the last two points of each sweep with a five-point average. The five-point average is found by considering the point to be replaced and its four surrounding points and finding the average of these five points. That is,

$$\hat{x}(n,1) = \frac{1}{5}\,[x(n-1,M-1) + x(n-1,M) + x(n,1) + x(n,2) + x(n,3)]$$

$$\hat{x}(n,2) = \frac{1}{5}\,[x(n-1,M) + x(n,1) + x(n,2) + x(n,3) + x(n,4)]$$

$$\hat{x}(n,M-1) = \frac{1}{5}\,[x(n,M-3) + x(n,M-2) + x(n,M-1) + x(n,M) + x(n+1,1)]$$

$$\hat{x}(n,M) = \frac{1}{5}\,[x(n,M-2) + x(n,M-1) + x(n,M) + x(n+1,1) + x(n+1,2)]$$

where $\hat{x}(n,m)$ is the replacement value for $x(n,m)$.

Once again the sequence is assumed to be cyclic when the replacement values for the first two points of the first sweep and the last two points of the last sweep are calculated.

Figures 6.1 and 6.2 illustrate the effects of the ad hoc smoothing methods on worst case and best case range spreading.

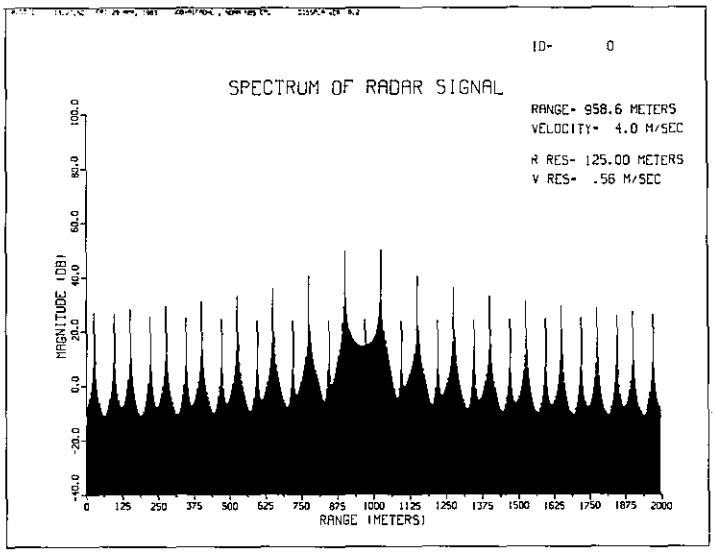

Figure 6.1.--Effect of smoothing on worst-case range spreading.

Figure 6.1a.--Unmodified.

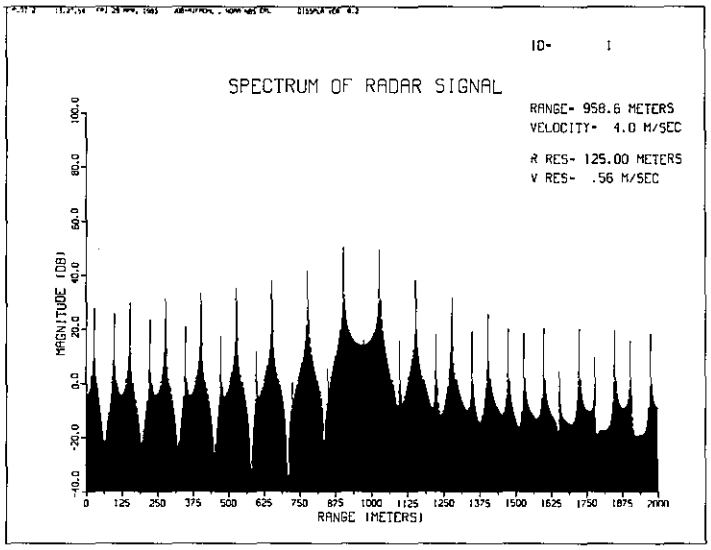

Figure 6.1b.--Smoothing method: Three-point average of two points.

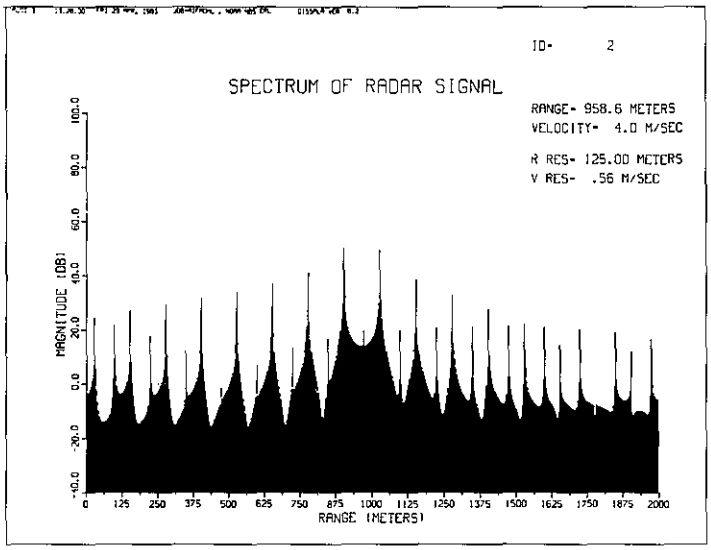

Figure 6.1c.--Smoothing method: Five-point average of two points.

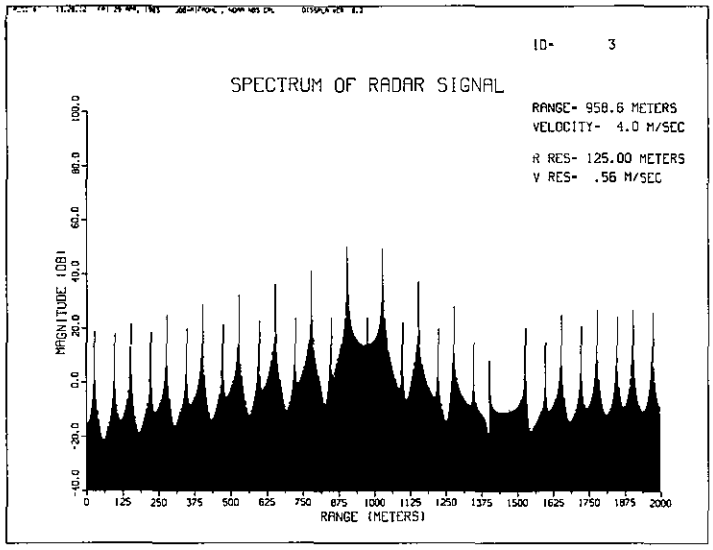

Figure 6.1d.--Smoothing method: Three-point average of four points.

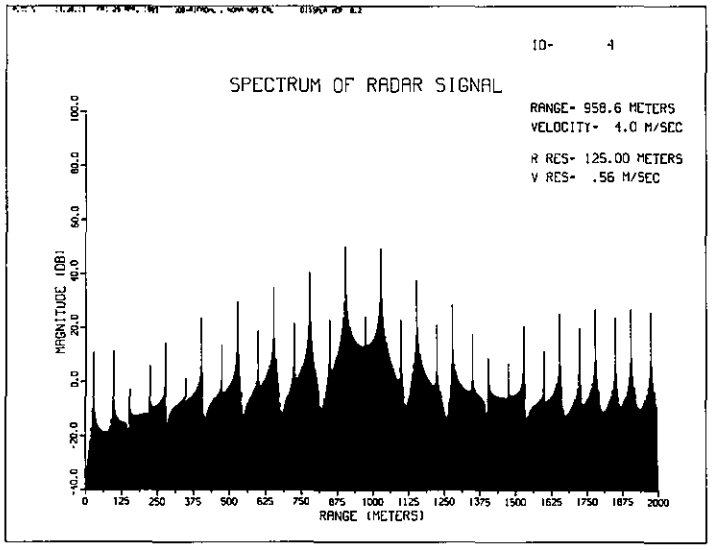

Figure 6.1e.--Smoothing methods: Five-point average of four points.

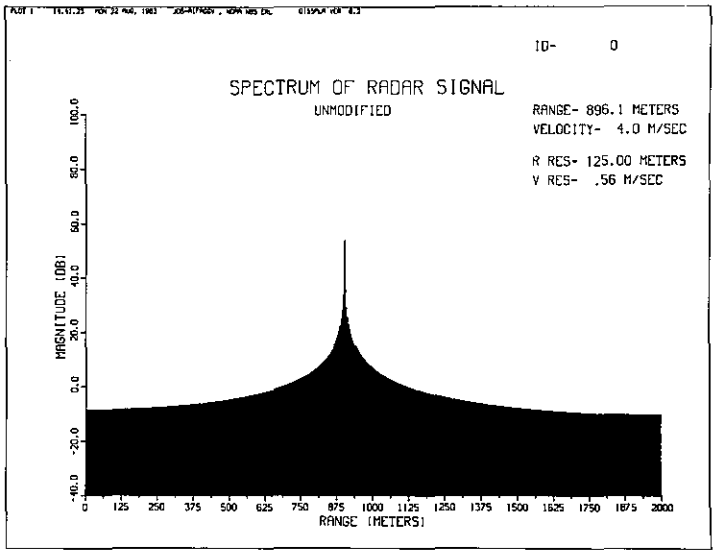

Figure 6.2.--Effect of smoothing on best case range spreading.

Figure 6.2a.--Unmodified.

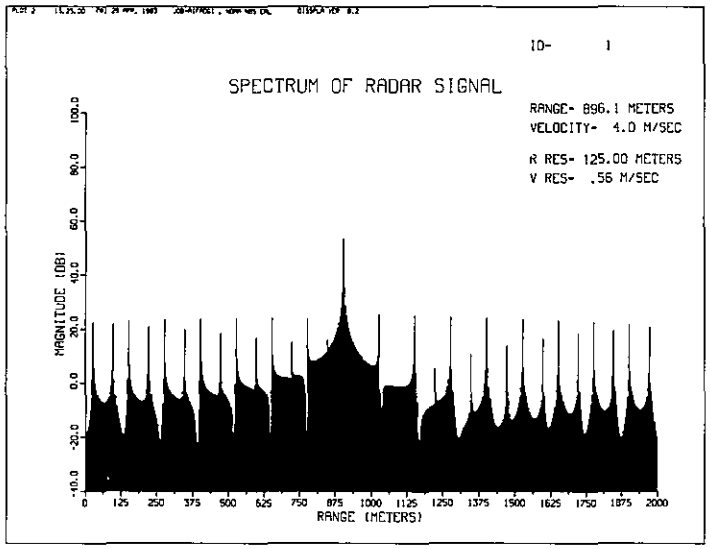

Figure 6.2b.--Smoothing method: Three-point average of two points.

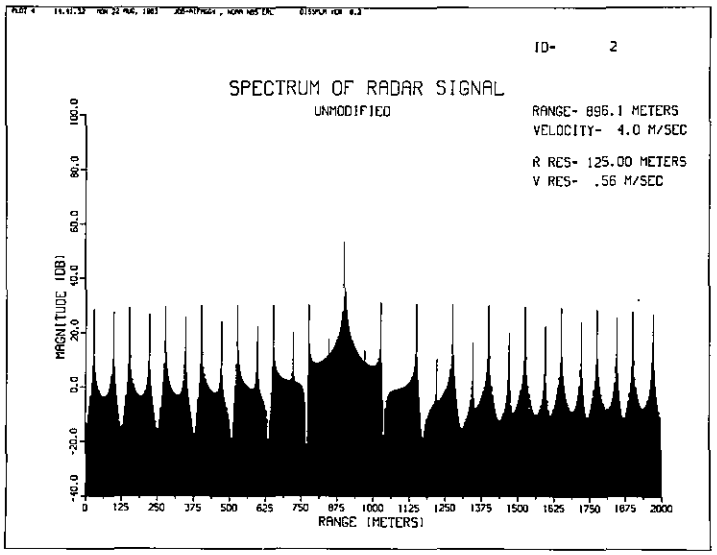

Figure 6.2c.--Smoothing method: Five-point average of two points.

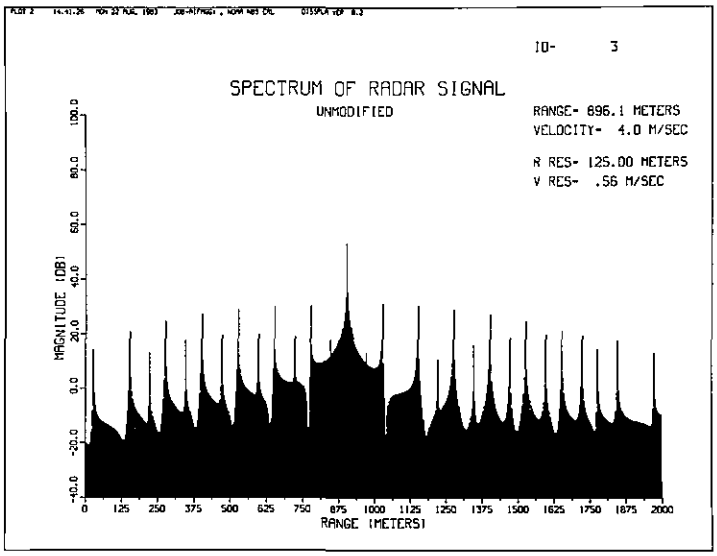

Figure 6.2d.--Smoothing method: Three-point average of four points.

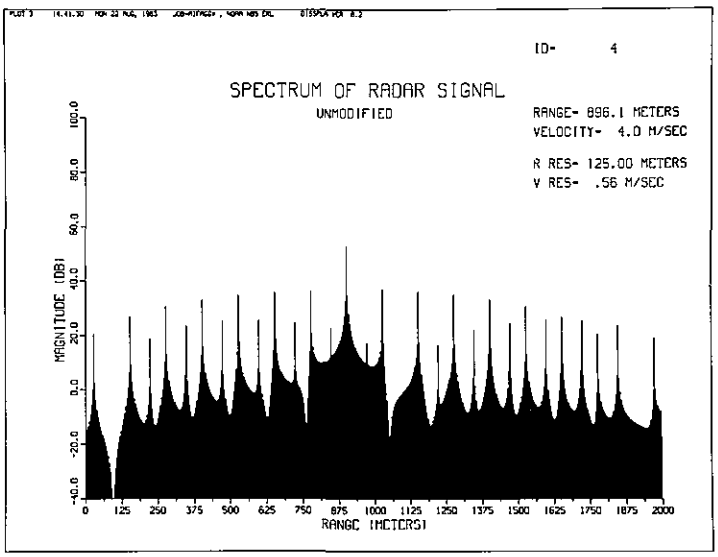

Figure 6.2e.--Smoothing method: Five-point average of four points.

7. CONCLUSIONS

Regardless of the method of processing, range spreading is a serious problem in the FM-CW radar. The problem is caused by the high sidelobes of the range spectrum. Windowing, is very effective in reducing sidelobe level, and hence range spreading, but has the undesirable effect of broadening the mainlobe of the range spectrum and thereby decreasing the effective range resolution.

A second method of reducing sidelobes consists of modifying a few data points at the discontinuity in the time series. The results of this method are not promising. There is slight reduction in range spreading in some portions of the spectrum, but overall, no significant improvement.

Through careful consideration of a radar's use, an appropriate window can be chosen. For instance, in a case where large resolution is not a critical

factor, but high sidelobe level is, the three-term Blackman-Harris window could be used. It would broaden the mainlobe greatly, but all sidelobes would be at least 60 dB down, a good trade under the circumstances. When range resolution is critical, the Riesz window is a good candidate. Its mainlobe is not much broader than that of the rectangular window and its first sidelobe is approximately 20 dB down. In addition, the rolloff is better than that of a rectangular window.

It is not clear at this point whether 1-D or 2-D processing is better. The 1-D method is currently in use and has given very good results. It has the advantage that just one DFT is needed over the entire sequence (depending on equipment available for processing the data, this may be the determining factor), and the results are in a good format for display purposes. It has the disadvantage that it weights the velocity spectrum unevenly across a range cell, thereby distorting it, whereas the 2-D method weights the entire range cell evenly.

8. REFERENCES AND ADDITIONAL READING

Barrick, D. E., 1973. FM/CW radar signals and digital processing. NOAA Technical Report ERL 283-WPL 26, NOAA Environmental Research Laboratories, Boulder, Colo., 22 pp.

Chadwick, R. B., and E. E. Gossard, 1983. Radar remote sensing of the clear atmosphere - Review and Applications. Proc. IEEE 71:738-753.

Chadwick, R. B., K. P. Moran, R. G. Strauch, G. E. Morrison, W. C. Campbell, 1976. A new radar for measuring winds. Bull. Am. Meteorol. Soc. 57:1120-1125.

Chadwick, R. B., K. P. Moran, W. C. Campbell, E. B. Earnshaw, and T. R. Detman, 1981. Development of a clear air radar to detect meteorological hazards at airports. AFGL-TR-81-0268, Air Force Geophysical Laboratory, Hanscom AFB, Mass.

Gossard, E. E., R. B. Chadwick, W. D. Neff, K. P. Moran, 1982. The use of ground based Doppler radars to measure gradients, fluxes and structure parameters in elevated layers. J. Appl. Meteorol. 21:211-226.

Harris, F. J., 1978. On the use of windows for harmonic analysis with the Discrete Fourier Transform. Proc. IEEE 66:51-83.

Rabiner, L. R., and B. Gold, 1975. Theory and Application of Digital Signal Processing. Prentice-Hall, Englewood Cliffs, New Jersey, 720 pp.

Richter, J. H., 1969. High-resolution tropospheric radar sounding. Radio Sci. 4:1261-1268.

Strauch, R. G., 1976. Theory and application of the FM-CW Doppler radar. Thesis for the Doctor of Philosophy Degree, University of Colorado, Boulder.

Appendix: Derivation of Mixed Signal

This derivation is valid only for the period of time during which the transmitted signal and received signal are being swept. That is, for $\tau < t_n < T$ the transmitted signal is

$$S_T(n,t_n) = A \cos 2\pi \left[\left(f_o + \frac{B}{2T} t_n \right) t_n + \phi_n \right] . \qquad (A.1)$$

The received signal is

$$S_R(n,t_n) = \tilde{A} \cos 2\pi \left\{ \left[f_o + \frac{B}{2T} (t_n - \tau) \right] (t_n - \tau) + \phi_n \right\} . \qquad (A.2)$$

The relationship for mixing two signals is

$$\cos\alpha \cos\beta = \frac{1}{2} \cos(\alpha-\beta) + \frac{1}{2} \cos(\alpha+\beta) .$$

When this identity is applied to (A.1) and (A.2), and the result is low-pass filtered, the frequency of the final signal will be the difference between the original frequencies. That is,

$$x(n,t_n) = \tilde{A} \cos 2\pi [\phi(n,t_n)] \qquad (A.3)$$

where

$$\phi(n,t_n) = f_o\tau - \frac{B}{2T} (\tau^2 - 2t_n\tau).$$

But

$$\tau = \frac{2R_o}{c} + \frac{2v}{c} nG + f_o \left(\frac{2v}{c} \right) t_n .$$

When this expression is substituted for τ, and terms containing $\frac{1}{c^2}$ are dropped,

$$\phi(n,t_n) = f_o \frac{2R_o}{c} + nf_o \frac{2v}{c} G$$

$$+ f_o \frac{2v}{c} + \frac{B}{T} \frac{2R_o}{c} + \frac{B}{T} \frac{2v}{c} nG \; t_n + \frac{B}{T} \frac{2v}{c} t_n^2 . \qquad (A.4)$$

Consider these terms of (A.4):

(a) $\frac{B}{T}\left(\frac{2v}{c}\right) nG\ t_n$

(b) $\frac{B}{T}\left(\frac{2v}{c}\right) t_n^{\,2}$.

These are maximum when $t_n = T$, so the maximum values are

(a) $B\left(\frac{2v}{c}\right) nG$

(b) $B\left(\frac{2v}{c}\right) T$.

For typical radar parameters, the terms are comparatively small and can be dropped. These are typical parameters:

$f_o \approx 3 \times 10^9$ Hz

$B \approx 10^6$ Hz

$T \approx G \approx 10^{-3}$ s

$c \approx 3.0 \times 10^8$

$R_o \approx 10^3 - 10^4$ m

$v \approx 1 - 10$ m/s

Thus, when $\tilde{A}$ is normalized to 1.0, the final expression for the mixed signal is

$$x(n,t_n) = \cos 2\pi\ [\phi(n,t_n)]$$

$$\phi(n,t_n) = \left[f_o\left(\frac{2R_o}{c}\right) + nf_o\left(\frac{2v}{c}\right) G\right] + \left[f_o\left(\frac{2v}{c}\right) + \frac{B}{T}\left(\frac{2R_o}{c}\right)\right] t_n \ .$$

☆ U.S. GOVERNMENT PRINTING OFFICE:1984—776-001 / 4112